AD_____

Award Number: DAMD17-98-1-8016

TITLE: Preliminary Investigation of the Role of Cellular Immunity in Estrous Cycle Modulation of Post-Resection Breast Cancer Spread

PRINCIPAL INVESTIGATOR: William J. M. Hrushesky, M.D.

CONTRACTING ORGANIZATION: Dorn Research Institute
Columbia, South Carolina 29209

REPORT DATE: August 2004

TYPE OF REPORT: Final

PREPARED FOR: U.S. Army Medical Research and Materiel Command
Fort Detrick, Maryland 21702-5012

REPORT DOCUMENTATION PAGE

Form Approved
OMB No. 074-0188

1. AGENCY USE ONLY (Leave blank)	2. REPORT DATE	3. REPORT TYPE AND DATES COVERED
	August 2004	Final (20 Apr 1998 - 3 Jul 2004)

4. TITLE AND SUBTITLE
Preliminary Investigation of the Role of Cellular Immunity in Estrous Cycle Modulation of Post-Resection Breast Cancer Spread

5. FUNDING NUMBERS
DAMD17-98-1-8016

6. AUTHOR(S)
William J. M. Hrushesky, M.D.

7. PERFORMING ORGANIZATION NAME(S) AND ADDRESS(ES)
Dorn Research Institute
Columbia, South Carolina 29209

E-Mail: William.hrushesky@med.va.gov

8. PERFORMING ORGANIZATION REPORT NUMBER

9. SPONSORING / MONITORING AGENCY NAME(S) AND ADDRESS(ES)
U.S. Army Medical Research and Materiel Command
Fort Detrick, Maryland 21702-5012

10. SPONSORING / MONITORING AGENCY REPORT NUMBER

11. SUPPLEMENTARY NOTES

12a. DISTRIBUTION / AVAILABILITY STATEMENT
Approved for Public Release; Distribution Unlimited

12b. DISTRIBUTION CODE

13. ABSTRACT (Maximum 200 Words)

The timing of resection of a transplantable breast cancer within the mouse's estrous cycle affects whether the cancer metastasizes or whether the operation cures the mouse. Surgery during the proestrus phase cured two and a half times more frequently than the opposite timing. We have studied the immune capacity of the mouse to generate natural killer (NK) cell activity. Surgical curability was optimal during proestrus when immunocompetence was most robust. Enhancing NK function diminishes metastatic spread while interfering with NK function increases spread. Estrogens diminish NK function. We will determine: whether hormone dependent immunocyte suppression affects fertility cycle modulation of cancer spread, which female sex hormone(s) control(s) post resection spread, whether estrogen and/or progesterone affect duration of NK cell activity suppression and numbers of NK, helper T, and/or suppressor T cells following resection, and whether deleting specific immune cell types by *in vivo* administration of antibodies abrogates the estrous cycle and sex hormone modulation of post resection cancer spread. Demonstration that NK, T helper and/or T suppressor cells are essential for sex hormone modulation of cancer spread, would implicate neoadjuvant sex hormone, and other cellular immune enhancement strategies before and/or following breast cancer resection in order to improve cure frequency.

14. SUBJECT TERMS	15. NUMBER OF PAGES
Surgery, neoplasm, estrous cycle, cellular immunity, chronobiology	53
	16. PRICE CODE

17. SECURITY CLASSIFICATION OF REPORT	18. SECURITY CLASSIFICATION OF THIS PAGE	19. SECURITY CLASSIFICATION OF ABSTRACT	20. LIMITATION OF ABSTRACT
Unclassified	Unclassified	Unclassified	Unlimited

Table of Contents

Final Report

Preliminary Investigation of the Role of Cellular Immunity in Estrous Cycle Modulation of Post-resection Breast Cancer Spread.

W. Hrushesky, S. You, Yin Xiong, M. Kobayashi, P. Wood, M.D.s
W.J.B. Dorn Veterans Affairs Medical Center
Columbia, SC 29209
william.hrushesky@med.va.gov

Introduction:

We have found that the timing of breast cancer resection within the mouse's and the women's fertility cycle determines whether or not that operation cures the mouse or woman or whether the cancer spreads throughout the hosts. This project proposed to determine the effect of manipulating the hormonal milieu by removal of the ovaries, or by ablation of the sex hormones in intact mice, on this biology. It also proposed to determine whether and how cellular immunity is altered differentially by resection at specific stages within the estrous cycle. The ultimate goal is to use the understanding generated to develop a peri-surgical therapy to increase the chances of curing this disease in thousands of premenopausal women who find themselves in this clinical situation each year. During this reporting period we have made good progress toward this goal.

Body:

Technical Objective #1: Establish tumors, followed by surgical resection of tumors in mice at each of four estrous cycles and/or *in vivo* hormonal modulations, followed by determination of metastatic recurrence. We proposed five tasks "Task #1-5" in this objective.

Task 1- Resect tumors in intact mice at one of four fertility cycle stages with no hormone modulation; follow up tumor recurrence with lung metastasis to examine fertility cycle influence on surgical breast cancer cure. **This task has been accomplished.**

Synopsis of Work Accomplished: Our previous studies demonstrated that estrous cycle stages just prior and near to ovulation to be superior, while those stages farther from ovulation were disadvantageous times for surgery. Data from this current series of experiments confirm the role of the estrous cycle in post-resection metastatic spread. A primary, transplantable, mammary carcinoma, which metastasizes to the lungs, was resected for surgical cure in cycling female mice at each fertility cycle stage. A group of oophorectomized (ovx) animals was also studied. In two independent studies, when resecting early stage cancers, a 96% surgical cure frequency was documented when the tumor was resected during estrus. The second best surgical cure rate was achieved when tumors were resected during metestrus (79% overall cure rate). Cure frequency in ovx animals was intermediate. We conclude that the timing of surgical resection within the estrous cycle affects the cancer's metastatic potential and that the optimal timing of resection may also depend to some extent upon the size (stage) of the resected cancer.

Task 2- Resect tumors in ovx mice with no hormone modulation. **This task has been accomplished.** See above synopsis.

Tasks 3 and 4- Ablate hormones (estrogen, progesterone) in ***intact and ovx*** mice with tumors using pellets with ICI 182780, RU486 -> Resect tumors -> Follow up tumor recurrence with lung metastasis. **These tasks have been accomplished.**

Synopsis of Work Accomplished: We established a stable breast cancer cell line, designated MTCL

that maintains fertility cycle cancer biology of the parent tumor (MTP). *In vitro* exposure of MTCL cells to progesterone indicated an inhibition by progesterone on MTCL cellular DNA synthesis; while exposure of the cells to a high dose of estrogen for 48 hours caused an increase of ^{3}H-thymidine uptake. We inoculated MTP or MTCL tumor cells into cycling female C_3HeB/FeJ mice and demonstrated that the post resection metastatic recurrence of MTCL tumors, like the original MTP tumors, depended upon the time of tumor resection within the mouse estrous cycle. Equivalent levels of sex hormonal receptors, epithelial growth hormonal receptors, tumor suppressors, and cell apoptosis relevant protein were found in these *in vivo* tumors, except that the cyclin E protein was significantly higher in MTP tumor cells compared to that in MTCL tumor cells. Our results indicate that MTCL cells retain many of biological features of the original MTP primary tumor cells, and, to our knowledge, is the first *in vitro* cell line that has been shown to maintain the unique estrous cycle dependence of *in vivo* cancer metastasis. (see appendix b).

We established a stable GFP (Green Fluorescent Protein) transfected MTCL cell line to study cancer chronobiology. GFP-expressing tumor cells can emit bright fluorescent light and the light signal is strong enough so that the external images of GFP-expressing tumors can be obtained using whole-body imaging technique. This technique is especially helpful in studying early stages of tumor metastasis. We succeeded in transferring a GFP expressing gene vector into MTCL tumor cells, and have passed this GFP tumor cell line over 10 generations *in vitro* with the percentage of green tumor cells maintained at about 95%. To test how long the GFP expression would last *in vivo*, we injected the cells subcutaneously onto the backs of female mice. We demonstrated that the expression of GFP in the MTCL tumor cells lasts about two months *in vivo* (three *in vivo* passages). In another experiment, we injected GFP-MTCL tumor cells into female mice and sacrificed the mice at different days after tumor injection and multiple organs were dissected. The third day after tumor cell injection, the GFP MTCL tumor cells were found in every organ we examined.

Task 5- Elevate hormone levels in ovx mice using pellets with estradiol, progesterone or prolactin prior to tumor transplantation-> Resect tumors-> Follow recurrence with lung metastasis. **This task has been accomplished.**

Technical Objective #2: To conduct cellular immune studies in intact and ovx tumor bearing, sex hormone-repleted mice before surgical resection, and four different times following surgical resection.

Tasks 6 and 7- Resect tumors in *intact and ovx* mice at one of four fertility cycle stages-> Follow up cellular immune response assays (NK cell assays and T cell subset determinations) on day 14 (pre-op) and post-op days 17, 20, 23 and 26. We resected tumors from intact and ovx mice at one of four fertility cycle stages. We accessed the cellular immune function of the tumor tissues, and have analyzed the gene expression profiles in the tumor tissues. **These tasks have been accomplished.**

Synopsis of Work Accomplished: We transplanted MPT4 mouse mammary tumor cells into 83 intact and 18 ovx female mice and resected these tumors two weeks later, for cure. After tumor removal, about half of the mice developed a lethal locally recurrent tumor at the surgical site. Those which did not (35/83-normal female and 10/18-ovx) were sacrificed when 5% of them had died from lung metastases. Surgical cure was highest when cancers were resected during estrus and lowest when they were resected during diestrus ($p<0.01$). We then created tissue microarrays from these tumors to assay for proteins related to cellular immune function, tumor growth, DNA repair and apoptosis, sex hormone sensitivity, and metastatic spread. Bcl-xs (pro-apoptosis) and BRCA1 (a DNA repair factor) were each expressed most robustly within tumors resected at estrus, and were lowest in tumors resected at diestrus. Conversely, expression of cathepsin L, a protein associated with metastatic spread, peaked in tumors resected at diestrus, and was weakest at estrus. These

changes of tumor cell protein expression may be responsible for the cycle's coordination of breast cancer growth and post-resection metastatic potential.
Another investigation focused on the relevance of the sex hormonal milieu/menstrual cycle stage to tumor metastatic spread. In a group of 26 mice, local (leg) MTP tumors were established. Following resection, mice were sacrificed and the incidence of tumor recurrence was evaluated. There was a 100% cure frequency (i.e. no lung metastases) in mice when their tumors were resected during the estrus phase *vs.* 28.5% cure rate when tumors were resected during the diestrus phase (P=0.0269). We also conducted cDNA microarray-based gene expression analyses on this tumor tissue to define all possible genes, which are either turned on or off by changing the sex hormonal milieu/estrous cycle stage. To solve the problem of tumor cell heterogeneity, we established a protocol for laser microdissection of tumor cells. We isolated RNA from the microdissected tumor cells via PCR amplification using known genes as targets (i.e. Her2/neu, S16). We compared the gene expression profile of one MTP tumor, dissected from a mouse at estrus stage and cured after tumor removal, with that of another MTP tumor, dissected from another mouse at diestrus that later died from lung metastases. To study the genes that are known to be relevant to metastatic spread and immune function, we are constructing our own oligo DNA microarray chip, which contains two hundred of these genes we are interested in.

Technical Objective #3: Determination of the effect of depleting NK and/or T suppressor cells and/or T helper cells upon the hormone dependence of post resection cancer spread. *Grant Transfer and No Cost Extension was requested and granted (Years 2 and 3) to accomplish tasks 8 and 9.*
Task 8- Perfect dose and schedule of antibody administration that ablates NK function (asialo GM-1) and depletes NK cell numbers, T helper cell (CD4), and T suppressor cell (CD8) numbers. Administer these antibodies prior to and following resection at each fertility cycle phase (P,E,M and D) and determine the effects of these immunocyte manipulations upon cure frequency and metastatic burden. **We were able to accomplish Task 8 in a slightly different way than proposed, because we found that not all of the antibodies were available, and the amount and especially the cost of the antibodies needed to conduct and complete this series of experiments were prohibitive in terms of the scope of the budget for this funding period. We instead made the decision to approach the question of hormone-dependence of post resection cancer spread using a different methodology.**
Synopsis of Work Accomplished: We determined which arms of the cellular immune system were the most important potential modulators of the prevention and /or facilitation of post-resection metastatic cancer spread by examining the nature and number of T cells, macrophages, and Natural Killer (NK) cells infiltrating each resected tumor. We did this by preparing tissue microassays from every tumor resected. We then stained these tissue samples immunohistochemically in order to identify each type of infiltrating host immunocyte. We utilized image-analysis software to objectively quantify the number of specific immunocytes (i.e. the density of specific immunocytes) in each tissue core sample. We are now correlating outcome (cure vs. recurrence) with the numbers of each of these types of immunocytes to see if cured tumors are associated with specific numbers and/or kinds of infiltrating immunocytes. These data are also being analyzed as a function of the estrous cycle phase at the time of resection in order to determine whether the *pattern* of immunocyte infiltration is an important characteristic in explaining the dependence of cure upon the timing of tumor resection within the estrous cycle.
Task 9- Ongoing and interim data analysis with preparation of data for presentation at cancer meetings (AACR), USAMRMC conference and manuscript(s) preparation and submission. Interim data analysis with preparation of data for presentation at cancer meetings and USAMRMC conference. **This task has been accomplished.**

Synopsis of Work Accomplished: Throughout the five year funding period (includes an approved two year no cost extension) we have been very active in writing and submitting manuscripts, with many already published or accepted for publication (see "Key Research Accomplishments" and "Reportable Outcomes"), and presenting data from these experiments at prestigious cancer conferences. Presentations are listed below:

2000 Annual meeting of American Association for Cancer Research (AACR): Bove, K, Lincoln, D, Wood, P, **Hrushesky, W**. Reproductive cycle coordination of tumor growth and post-resection local recurrence of a low metastatic potential, gene marked, breast cell line.

2000 Seventh Meeting Society for Research on Biological Rhythms, Amelia Island Plantation, Jacksonville, Florida: Wood P, Bove K, **Hrushesky W**. Meaningful and reproducible reproductive cycle modulation of cancer biology.

2002 September, Era of Hope DoD Breast Cancer Research Program Meeting, Orlando, Florida: **Hrushesky WJM,** You S, Kobayashi M., Wood P. Fertility Cycle Coordinates Molecular Pathways Responsible for Cancer Growth and Spread.

2002 October, 7th Annual VA National Cancer Symposium, Alexandria, Virginia: Wood P, You S, **Hrushesky WJM**. Fertility Cycle Coordinates Molecular Pathways Responsible for Cancer Growth and Spread.

2003 April, 94th Annual AACR Meeting, Toronto, Canada: You S, Kobayashi M, Wood P, Xu Y, Musk P, **Hrushesky W**. Mouse Mammary Circadian Rhythm and mPER1 Gene Expression.

2004 March AACR 2004, Orlando, Florida: You S, Li W, Kobayashi M, Xiong Y, **Hrushesky W**, Wood P. Creation of a stable breast cancer cell line that maintains fertility cycle cancer biology of the parent tumor.

2004 June, American Society of Clinical Oncologists (ASCO), New Orleans, Louisiana: Demicheli R, Bonadonna G, **Hrushesky W**, Moliterni A, Retsky M, Valagussa P, Zambetti M. The timing of breast cancer recurrence after mastectomy and adjuvant CMF chemotherapy supports a dormancy-based model for metastatic development.

Key Research Accomplishments: (Since last annual report)

- Collaboration with Philip Buckhaults, Ph.D., a co-investigator on the SAGE Gene Expression grant award, and his research group at Univ. of South Carolina, to work in this area
- Recruitment of Dr. Ohmori, M.D., Ph.D. from Japan to work in this area (publication attached)
- Mentored peer reviewed funding of Dr Shaojin You's NIH RO3 grant-2004.
- Recruitment of PhD student Mei Li and Masters student Peter Miller to work in this area.

New Grants

- DoD Concept Award: SAGE Gene Expression Profiles Characterizing Cure – profiling RNA expression to determine the effects of sex hormonal milieu (P, E, M and D) upon cure frequency and metastatic burden.

In Press

- Shaojin You, Patricia A Wood, Yin Xiong, Minoru Kobayashi, Jovelyn Du-Quiton, and William J.M. Hrushesky. Daily Coordination of Cancer Growth and Circadian Clock Gene Expression. Breast Cancer Research and Treatment 00:1-14, 2004 (see appendix a)
- Shaojin You, Wei Li, Minoru Kobayashi, Yin Xiong, William Hrushesky, Patricia Wood. Creation of a Stable Breast Cancer Cell Line That Maintains Fertility Cycle Cancer Biology of the Parent Tumor. In Vitro Cell Dev Biol Anim. 2004 Mar 1 (see appendix b)

Submitted for Publication

- Wood P., Hrushesky W. Sex Cycle Modulates Cancer Growth (submitted to Breast Cancer Research and Treatment, Dec 2004-see appendix c)
- Bove K., Wood P., Chambers A., Hrushesky W. Molecular Mediators of Angiogenesis are Modulated by the Fertility Cycle in Normal Mammary Tissue and in Mammary Tumor. (submitted to Breast Cancer Research and Treatment-Dec 2004)
- Hrushesky W. Improbability of the metastatic cascade. Perspectives in Biol and Med.
- Baum M., Demicheli R., Hrushesky W., Retsky M. Does Surgery Unfavorably Perturb the "Natural History" of Early Breast Cancer by Accelerating the Appearance of Distant Metastasis? (submitted to Eur J Ca, Oct 2004)
- Demicheli R., Rosalba M., Hrushesky W. Breast Cancer Recurrence Dynamics Following Adjuvant CMF is Consistent with Tumor Dormancy and Mastectomy-driven Acceleration of the Metastatic Process (submitted to Breast Cancer Research and Treatment-Dec 2004)

Reportable Outcomes: (* Since last annual report 2003)

Publications:

1) Hagen A, Hrushesky W. Menstrual timing of breast cancer surgery. Am J Surg 1998;104:245-261.

2) Hrushesky W, Vyzula R, Wood P. Fertility maintenance and 5-fluorouracil timing within the mammalian fertility cycle. Reprod Toxicol 1999;13:413-420.

3) Hrushesky W, Lester B, Lannin D. Circadian coordination of cancer take and metastatic spread. Int J Can 1999;83:365-73.

4) Hrushesky W. Rhythmic Menstrual Cycle Modulation of Breast Cancer Biology. J Surg Oncol 2000; 74: 238-241.

5) Retsky M, Demicheli R, Hrushesky, W. Premenopausal Status Accelerates Relapse. *BREA* 65 (3), 217-224, February/March, 2001.

6) Retsky M, Demichelli R, Hrushesky WJM. Wounding from Biopsy and Breast Cancer Progression. Letter to *The Lancet,* Vol 357, No 9261, 31 Mar 01, page 1048.

7) Bove K, Lincoln D, Wood P, Hrushesky WJM. Fertility cycle influence on surgical breast cancer cure. Breast Cancer Research and Treatment 75:65-72, 2002.

***8)** Demicheli R, Bonadonna G, Hrushesky W, Retsky M, Valagussa P. Menopausal status dependence of early mortality reduction due to diagnosis of smaller breast cancer (T1 v T2-T3): Relevance to Screening. J Clin Oncol 22(1):102-107, Jan 2004.

***9)** Retsky M, Bonadonna G, Demicheli R, Folkman J, Hrushesky W, Valagussa P. Hypothesis: Induced angiogenesis after surgery in premenopausal node-positive breast cancer patients is a major underlying reason why adjuvant chemotherapy works particularly well for those patients. Breast Cancer Res 2004, 6:R372-R374.

***10)** Demicheli R, Bonadonna G, Hrushesky W, Retsky M, Valagussa P. Menopausal Status Dependence of the timing of breast cancer recurrence after surgical removal of the primary tumour. Breast Cancer Research 2004 (6): R689-R696.

Abstracts:

Hrushesky W, Wood P, Bove K. Mammalian fertility cycles modulate cancer growth and spread. 3rd Annual VA Oncology Cancer Symposium. San Antonio, TX, 1998.

Bove, K, Wood, PA, Hrushesky W. Vascular endothelial growth factor (VEGF) and basic fibroblast growth factor (bFGF) expression in breast cancer varies with fertility cycle stage. Proc AACR 40: 1999.

Bove, K, Wood, P, Hrushesky, W. Molecular mediators of angiogenesis are modulated by the

fertility cycle in breast cancer (abstract). Joint meeting of the eighth international conference of chronopharmacology and chronotherapeutics and the american association for medical chronobiology and chronotherapeutics, Williamsburg, VA, 1999.
Hrushesky W, Bove K, Wood P. Breast cancer resection within the menstrual cycle: risks, costs and benefits. 1st Milan Breast Cancer Conference. Milan, Italy, 1999.
Bove K, Wood P, Hrushesky W. Molecular mediators of angiogenesis are modulated by the fertility cycle in breast cancer. 4th annual VA oncology cancer symposium. Washington, DC, 1999.
Wood, P, Lincoln, D, Bove, K, Clark, R, Hrushesky W. Tumor thymidylate synthase (TS) activity and mRNA vary rhythmically throughout the day. Proc AACR 2000.
Bove, K, Lincoln, D, Wood, P, Hrushesky, W. Reproductive cycle coordination of tumor growth and post-resection local recurrence of a low metastatic potential, gene marked, breast cell line. Proc AACR 2000.
Hrusheksy W, Bove K, Chambers A, Wood P. Reproductive cycle and tumor stage affect measures of cell proliferation and angiogenesis. In: Breast Cancer Research Program, Era of Hope; 2000 June 8-12; Atlanta, GA; 2000.
Wood P, Bove K, Hrushesky W. Meaningful and reproducible reproductive cycle modulation of cancer biology. In: Seventh Meeting Society for Research on Biological Rhythms; 2000; Amelia Island Plantation, Jacksonville, Florida; 2000.
Kobayshi M, You S, Wood P, Rich I, Hrushesky WJM. Prominent Circadian and Estrous Cycle Impact upon Tumor Biology. Eighth Meeting of the Society for Research on Biological Rhythms. Amelia Island Plantation and Conference Center, Jacksonville, FL; May 22-26, 2002.
You S, Kobayashi M, Rich I, Musk P, Wood P, Hrushesky WJM. Tissue and cDNA Microarrays for High-Throughout Molecular Profiling of Cancer Chronobiology. Eighth Meeting of the Society for Research on Biological Rhythms. Amelia Island Plantation and Conference Center, Jacksonville, Florida; May 22-26, 2002.
Hrushesky WJM, You S, Kobayashi M., Wood P. Fertility Cycle Coordinates Molecular Pathways Responsible for Cancer Growth and Spread. Era of Hope 2002 DoD Breast Cancer Research Program Meeting, Orlando, Florida; September 25-28, 2002.
Wood P, You S, Hrushesky WJM. Fertility Cycle Coordinates Molecular Pathways Responsible for Cancer Growth and Spread. 7th Annual VA National Cancer Symposium, Alexandria, Virginia; October 2-4, 2002.

Conclusions:

During this five year grant period, we were successful in completing a series of exquisite experiments in order to understand the role of cellular immunity in estrous cycle modulation of post-resection cancer spread. We were able to further elucidate fertility cycle influence on surgical breast cancer cure by resecting an implanted breast cancer in intact, cycling mice and oophorectomized mice, and through hormonal manipulation (i.e. sex hormone ablation via pellets). We successfully established an *in vitro* tumor cell line; the first *in vitro* cell line to our knowledge that has been shown to maintain the unique estrous cycle dependence of *in vivo* cancer metastasis, in order to study the effects of sex hormone exposure on tumor cell proliferation and DNA synthesis. To better study cancer chronobiology, we also established a stable Green Fluorescent Protein (GFP) tranfected tumor cell line, an important whole body imaging technique for studying the early stages of tumor metastasis. We demonstrated how the fertility cycle coordinates molecular pathways responsible for cancer growth and spread by creating tissue microarrays from resected tumor tissue to assay for proteins related to cellular immune function, tumor growth, DNA repair and apoptosis, sex hormone sensitivity, and metastatic spread via immunohistochemical staining. Finally, in an

important series of experiments, we cryo-preserved tumor tissue resected at different estrous cycle stages and conducted cDNA microarray-based gene expression analyses to establish gene expression profiles of these tumors.

Our current research focus, first undertaken during this granting period, is on the genes that are relevant to tumor spread and immune function. To this end we have started construction of our own oligo DNA microarray chip, which will contain two hundred of the genes we are interested in studying. We found that not only is cellular immune function coordinated by the estrous cycle, but new blood vessel formation, tumor cell proliferation and apoptosis are each coordinated by this important biological rhythm. We are committed to identifying and putting together the pieces of this clinically important puzzle.

References:

Please see the "reportable outcomes".

Appendices:

a. Shaojin You, Patricia A Wood, Yin Xiong, Minoru Kobayashi, Jovelyn Du-Quiton, and William J.M. Hrushesky. Daily Coordination of Cancer Growth and Circadian Clock Gene Expression. Breast Cancer Research and Treatment 00:1-14, 2004 (In Press)
b. Shaojin You, Wei Li, Minoru Kobayashi, Yin Xiong, William Hrushesky, Patricia Wood. Creation of a Stable Breast Cancer Cell Line That Maintains Fertility Cycle Cancer Biology of the Parent Tumor. In Vitro Cell Dev Biol Anim. 2004 Mar (In Press)
c. Wood P., Hrushesky W. Sex Cycle Modulates Cancer Growth (submitted to Breast Cancer Research and Treatment, Dec 2004)

Breast Cancer Research and Treatment 00:1-14, 2004.

Daily coordination of cancer growth and circadian clock gene expression

Shaojin You, Patricia A Wood, Yin Xiong, Minoru Kobayashi, Jovelyn Du-Quiton, and William JM Hrushesky*
Medical Chronobiology Laboratory, Dorn Research Institute, WJB Dorn VA Medical Center, 6439 Garners Ferry Road, Columbia, SC. 29209, USA

Key words: Cancer, circadian, core clock genes, clock controlled genes, cancer growth, cancer proliferation

Summary

Background. Circadian coordination in mammals is accomplished, in part, by coordinate, rhythmic expression of a series of circadian clock genes in the central clock within the suprachiasmatic nuclei of the hypothalamus. These same genes are also rhythmically expressed each day within each peripheral tissue.

Methods.: We measured tumor size, tumor cell cyclin E protein, tumor cell mitotic index, and circadian clock gene expression in liver and tumor cells at six equispaced times of day in individual mice of a 12-hour light, 12-hour dark schedule.

Results. We demonstrate that C3HFeJ/HeB mice with transplanted syngeneic mammary tumor maintain largely normal circadian sleep/activity patterns, and that the rate of tumor growth is highly rhythmic during each day. Two daily 2.5 fold peaks in cancer cell cyclin E protein, a marker of DNA synthesis, are followed by two daily up-to-3-fold peaks in cancer cell mitosis (one minor, and one major peak). These peaks are, in turn, followed by two prominent daily peaks in tumor growth rate occurring during mid-sleep and the second, during mid-activity. These data indicate that all therapeutic targets relevant to tumor growth and tumor cell proliferation are ordered in tumor cells within each day. The daily expression patterns of the circadian clock genes *Bmal1, mPer1*, and *mPer2,* remain normally circadian coordinated in the livers of these tumor bearing mice. *Bmal1* gene expression remains circadian rhythmic in cancer cells, although dampered in amplitude, with a similar circadian pattern to that in normal hepatocytes. However, tumor cell *mPer1* and *mPer2* gene expression fails to maintain statistically significant daily rhythms.

Conclusion. We conclude that, if core circadian clock gene expression is essential to gate tumor cell proliferation within each day, then there may be substantial redundancy in this timing system. Alternatively, the daily ordering of tumor cell clock gene expression may not be essential to the daily gating of cancer cell DNA synthesis, mitosis and growth, indicating that host central SCN mediated neuro-humoro-behavioral controls and/or daily light induced changes in melatonin or peripherally induced rhythms such as that resulting from feeding effects, may be adequate for the daily coordination of cancer cell expression of proliferation related therapeutic targets.

Introduction

In mammals, most physiological, biochemical, and behavioral processes vary in a predictable periodic manner with respect to time of day for purposes of biologic economy and survival(1). The suprachiasmatic nuclei (SCN) have been recognized as the primary neurobiologic circadian pacemaker. The at least nine, *(Ck1, Clock, Per1, 2, and 3, Bmal1*, *Tim*, and *Cry1, 2*) core clock genes so far described, are responsible for circadian rhythms. These genes are rhythmically expressed within the SCN with oscillating feed forward and feed back dynamics, that set and reset circadian time daily to the temporal environment from photoperiodic and other rhythmic daily input(2-7). Each cell in most peripheral tissues is apparently connected to the SCN either through direct autonomic nervous connection and/or circadian organized hormonal signals, time-specific daily behaviors, and metabolic signals from meal timing (8, 9). These core clock gene loops are likewise expressed rhythmically within rodent and human peripheral tissues. It is not clear whether the daily coordinate expression of these genes in peripheral tissues is essential for organizing tissue functions each day. The peak timing of clock gene expression in each tissue is delayed by up to 6 hours with respect to the phase of the SCN daily rhythm(2, 10, 11). We hypothesize that these circadian clock genes coordinate essential cell functions in circadian time by coordinating the tissue specific

expression of circadian clock controlled genes which, in turn, gate these processes within each day in normal tissues, and that malignant tissues may exhibit abnormalities in these pathways.

The daily gating of cell cycle events in peripheral tissues, such as skin, to certain specific times of day has long been described in human beings(12). Epithelial cells of the human gut and hematopoietic precursor cells within the bone marrow of free living, genetically distinct, healthy individuals undertake the process of DNA synthesis non-randomly within each day(13, 14). This is important because the susceptibility of these two tissues to cytotoxic damage determines the toxic therapeutic ratio of most cancer treatments.

The timing, within the day, of cancer chemotherapy reproducibly affects the proportion of tumor bearing mice cured(15, 16). The toxicity of cancer chemotherapy, as well as the control of human cancer, has been improved by the optimal circadian timing of cancer chemotherapy(17, 18). This work has been confirmed by several randomized clinical trials(19, 20) and extensive animal studies(21, 22). More recently, we have demonstrated that this time of day-based anticancer drug selectivity exists, in part, because important proliferation associated drug targets, such as thymidylate synthase, are reproducibly more or less available at specific times each day(23, 24).

Murine and clinical experiments each clearly indicate that, while toxicity and dose intensity each depend on the circadian timing of cytotoxic agent delivery, a second dose-intensity-independent relationship also exists between circadian drug timing and optimal anticancer efficacy(25). Human cancer cell proliferation is also coordinated within each day. Mitotic figures of benign and malignant epidermoid cells from an environmentally synchronized patient appear and disappear rhythmically throughout each day(26). Non-Hodgkin's lymphoma cells removed from two dozen patients, around the clock, are more frequently engaged in DNA synthesis during each night(27). The daily peak in the percentage of S-phase diploid and aneuploid ovarian cancer cells among 35 patients with metastatic ovarian cancer, sampled round the clock, occurs most commonly in mid-morning. This timing offers an unique therapeutic opportunity for optimal circadian S-phase active chemotherapy timing in the morning to coincide with high ovarian cancer cell vulnerability (28).

In this study, we investigate to what extent circadian time keeping is intact in cancer bearing mice, and whether circadian coordination of cancer growth and concurrent cancer cell cycle traverse occurs. We also determine whether core circadian clock gene expression in tumors resected from animals at six equispaced times of day, is also organized during each day. We also determined whether the daily patterns of expression of circadian clock genes in tumor cells differs from normal liver cells from these same mice.

Method and Materials

Animals and Housing

Four to five week old female C3HeB/FeJ mice (C3H) were purchased from Jackson Laboratory (Bar Harbor, ME) and allowed to acclimate for two months prior to experimental procedures. Mice were housed in rooms with regular lighting schedule of 12 hours lights on alternating with 12 hours lights off (LD schedule). Time is referenced to Hours After Lights are On (HALO). All experiments were performed in compliance with the NIH Guide for Care and Use of Laboratory Animals and were approved by our VA Institutional Animal Care and Use Committee.

Tumor Cell Inoculation

A primary, syngeneic estrogen binding mammary tumor (MTP) arising spontaneously in female inbred C3H mice was obtained from Bernard Fisher (29) and passed in female C3HeB/FeJ mice as described(30). A single-cell suspension was prepared by mechanical dissociation of MTP tumor and $2x10^4$ viable tumor cells in 50ul RPMI medium were inoculated subcutaneously on the flank of female mice. These tumors, when unresected, continue to grow locally until the animal succumbs.

Effect of Tumor on Circadian Locomotor Activity

To assess general circadian organization of the tumor-bearing host, twelve mice were housed individually in cages with running wheels connected to computerized activity monitors for two weeks before tumor cell inoculation. Tumor cells were injected when the mice were accustomed to the wheels and had reached maximum activity levels. The voluntary locomotor activity of each mouse and its circadian pattern were recorded and analyzed (VitalView 3.1 and Actiview 1.2, Mini Mitter Co, Bend, OR 97701). Tumor was measured daily with calipers, with volumes calculated as length x width x height, at the same biological time each day, at the end of the daily activity span (10 HALO).

Effect of Circadian Time on Tumor Growth

In the first experiment, 54 mice were separated into three equal groups and housed in three different animal rooms, four per cage. MTP tumor cells were inoculated at one time of day (10 HALO) on day 1. Tumor size was measured once the tumor became measurable (about 10 days after tumor inoculation). To make tumor size measurements at six circadian times of a day without disturbing the mice too much, we scheduled the

"lights on" time in each of the three rooms 4 hours apart from one and another. Tumor size was measured twice a day in each mouse at a 12-hour interval, by the same individual. This allowed determination of tumor size and growth rate every 12 hours. In each of these three groups of mice, tumor

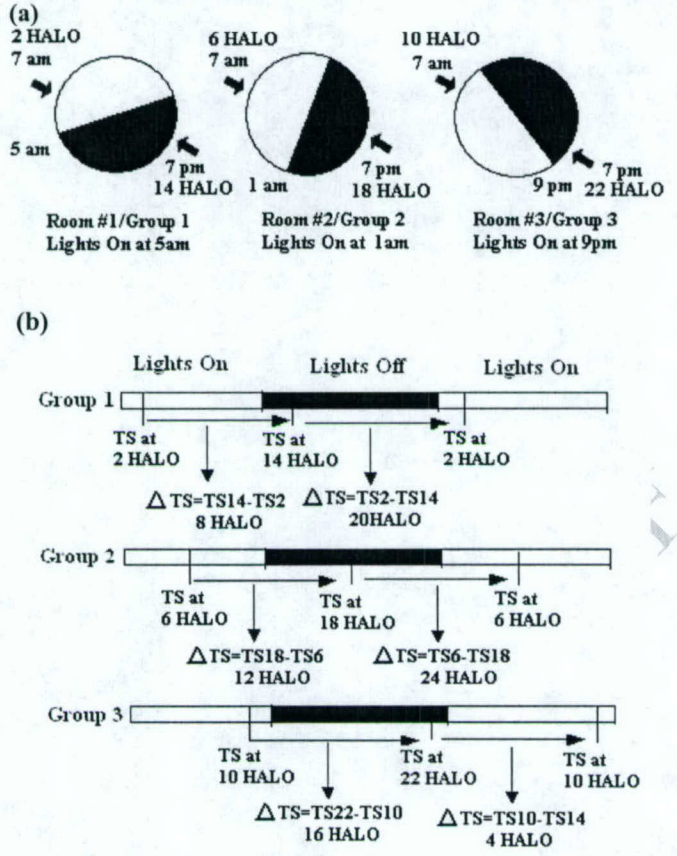

Figure 1. Animal study design with three different lighting schedules (12 hours dark,12 hours light) and twice daily tumor measurement schedules. Tumor size (TS) was measured twice daily in each mouse at 12 hour intervals in each group but at different circadian times between groups (a). TS was measured at 2 and 14 HALO (hours after lights on) in group 1, at 6 and 18 HALO in group 2, and at 10 and 22 HALO in group 3 mice. Changes in tumor size (ΔTS) were calculated in each mouse as the difference in tumor size over each successive 12-hour period which was then plotted at the circadian midpoint between each 12 hour interval (b).

was measured across three different 12 hour segments of each day (group 1 mice at 2 and 14 HALO, group 2 mice at 6 and 18 HALO, group 3 mice at 10 and 22 HALO) (**Figure 1a).** Equal groups of tumor bearing mice were euthanized at day 13 after tumor cell inoculation, when their tumors were in early-mid stage of growth. In the second experiment, 26 mice were housed in one room. Tumor size was measured twice a day at 2 and 14 HALO, similar to group 1 mice in the above study

Tumor Growth Rate at Each of Six Times of Day

Tumor growth rates during different circadian time spans were defined as the tumor size differences between two neighboring 12 hour measurements made Therefore, the series of tumor growth rates represents tumor growth over six different 12 hour circadian time spans. We assigned each growth rate to the mid point between each of these 12-hourly measurements to represent the change in tumor size (ΔTS) over each time interval (Figure 1b). For example, tumors in group 1 mice, measured twice a day at 2 and14 HALO on day 10, had tumor sizes of $TS10_{(2)}$ and $TS10_{(14)}$. The tumor growth rate between 2 and 14 HALO at day 10 is defined as $\Delta TS = TS10_{(14)}\text{-}TS10_{(2)}$. This particular tumor growth rate is represented at the mid point between 2 and 14 HALO, which is 8 HALO on day 10 (circadian mid point) as the average growth rate during this interval (change/averaged over this circadian time interval). With three groups of mice, this represents six different circadian mid points, which were 4, 8, 12, 16, 20, and 24 HALO, over which tumor growth rates were calculated.

Tumor and Liver Tissue Collection

After euthanasia, tumor and liver tissues were dissected from each mouse. One part of tumor and liver tissues were placed into liquid nitrogen and transferred to a -80^0C freezer. The remaining tissues were fixed by 10% buffered formalin for 24 hours and embedded in

paraffin block. The paraffin blocks were stored at 4^0C.

Tumor Mitotic Index

One hematoxylin & eosin stained (H&E) section was prepared from each tumor and evaluated under Axioskop microscope (Axioskop, Carl Zeiss, German). Areas containing the most viable tumor cells were selected for imaging. Ten consecutive images (approximately 300 to 400 tumor cells/image) were randomly taken from each section using 40x objective lens and the AxioCam Digital camera (Carl Zeiss, German). The images were viewed on the computer screen using Adobe Photoshop software and the number of mitotic figures in each image was counted. The average mitotic figure from ten images (mitotic index) from each tumor was calculated.

Tumor Tissue Array

A trained clinical and experimental pathologist examined H&E sections from each tumor and marked the most viable areas of the tumor tissue. These areas were aligned with the tumor specimen within each tissue block for tissue array core sampling. A tissue array instrument (Beecher Instrument Inc, Sun Prairie, WI) was used to sample and transfer the paraffin-fixed tissue cores into pre-drilled holes on a recipient paraffin block. For each tumor block, duplicate tissue cores, 0.6 mm diameter, were taken, labeled by position, and arrayed side by side in the recipient block. Multiple 5 um sections were cut from the array block and mounted on the positively charged glass slides (SurgiPath, Richmond, IL) for histopathologic and immunochemical examination.

Cyclin E Protein Immunohistochemistry

The histopathologically selected tissue array sections, after deparaffinization and hydration, were digested using proteinase K (20 ug/ml in PBS) for 20 minutes and washed in PBS twice (pH 7.2) for 5 minutes. Endogenous peroxidase activity was blocked by 3% H_2O_2 in PBS for 15 minutes. Slides were incubated in normal goat serum for 2 hours at room temperature. The primary antibody, rabbit polyclonal anti-cyclin E (1:2000, Santa Cruz Biotechnology, Santa Cruz, CA), was applied to sections and incubated overnight at 4^0C. The secondary antibody (goat anti-rabbit IgG) and AB complex (Vectastain ABC kit, Vector Laboratory Inc., Burlingame, CA) were applied for 30 minutes at room temperature, respectively. Between incubations, slides were washed three times (5 min/each) in PBS. The color was developed by 3, 3'-diaminobenzidine tetrahydrochloride (Peroxidase substrate kit DAB, Vector Laboratory Inc., Burlingame, CA). The sections were finally counterstained with Harris' hematoxylin (Sigma, St. Louis, MO). The same tissue array slides were stained without primary antibody as negative controls.

Quantitation of Cyclin E Immunostain

The immunostained tumor tissue array sections were viewed under the Axioskop microscope. One area, which represented the average level of the cyclin E protein stain signal and consisted of only viable tumor cells, was selected from each tumor tissue core. A digital image was taken from this area using AxioVision (Carl Zeiss, German) and analyzed using SigmaScan Pro4 (SPSS Inc. Chicago, IL). The target objectives in this image were defined and selected by a pre-set intensity. The average intensity of the objectives ($Obj_{intensity}$) was measured. The intensities ($Obj_{intensity}$) of the duplicate tissue cores were averaged ($M_{intensity}$). Images were also taken from the coordinated areas of the negative control stain sections to estimate background intensity ($B_{intensity}$). The final formula for calculating specific cyclin E immunostain intensity was:

$$M'_{intensity} = (\log 255 - \log M_{intensity}) - (\log 255 - \log B_{intensity}) \quad (31\text{-}33).$$

PECAM (CD 31) Immunohistochemistry and Tumor Blood Vessel Count

Tumor tissue array sections were stained with anti-PECAM antibody (rabbit polyclonal anti-PECAM diluted at 1:400, Santa Cruz Biotechnology, Santa Cruz, CA) using similar procedures (see cyclin E protein immuno-histochemistry). The PECAM positively stained tumor blood vessels were quantitatively evaluated under the Axioskop microscope with 40x objective lens. Numbers of tumor blood vessels in each tumor tissue core were counted and averaged between the duplicate tumor tissue cores.

Tumor and Liver RNA Isolation

Total RNA was isolated from the frozen tumor and liver tissues using Trizol reagent (InVitroGen, Carlsbad, CA). Briefly, the tumor and liver tissues (20-30mg) were homogenized in 5 ml Trizol reagent and mixed vigorously with 1 ml chloroform for 15 seconds. The mixtures were then centrifuged at 10,000 x g at 4^0C for 15 minutes. The aqueous phases were transferred to fresh tubes. Isopropyl alcohol was then added (2.5 ml/tube) and mixed well. The tubes were allowed to stand at room temperature for 20 minutes and then centrifuged at 10, 000 x g at 4^0C for 10 minutes. RNA pellets were washed with 5 ml pre-chilled 70% alcohol and dissolved in 50-100 ul of DEPC-treated water. The RNA concentration was determined using a spectrophotometer (SmartSpec™ 3000, BioRad Laboratories, Hercules, CA). All RNA

samples were checked for integrity by RNA agarose gel analysis.

RNA Reverse Transcription

To synthesize the first chain of the cDNA template, five micrograms of the total RNA was reverse-transcribed in a final volume of 20 ul reaction system, which contained M-MLV reverse transcriptase (InVitroGen., Carlsbad, CA), 1 mmol/L dNTPs, 40 U RNase inhibitor (Amersham Pharmacia Biotech, Freiburg, Germany), and 300 ng oligo d(T) 12-18 (InVitroGen., Carlsbad, CA). The reaction was performed at 37^0C for 50 minutes, followed by 70^0C for 15 minutes and 4^0C for 5 minutes.

Real-time PCR

Real-time PCR analyses were performed with an iCycler IQ Real-time PCR detection system (BioRad Laboratories, Hercules, CA). Intron-spanning primers were designed to meet specific criteria by using Primer Express software (Perkin Elmer, Foster City, CA). The primer pairs used for the amplification of each gene product were as follows:

mPer 1: 5'- CTGAGGAGGCCGAGAGGAAAGAA-3'
5'- AGGAGGAGGAGGCACATTTACGC- 3'
mPer2: 5'- GAGCAGGTTGAGGGCATTAC-3'
5'- TGGAGGCCACTTGGTTAGAG-3'
Bmal1: 5'- AAGGATGGCTGTTCAGCACATGA- 3'
5'-CAAAAATCCATCTGCTGCCCTG-3'
S16: 5'- AGGAGCGATTTGCTGGTGTGGA 3'
5'-GCTACCAGGGCCTTTGAGATGGA 3'

All PCR reagents were purchased from BioRad Laboratories. The total PCR reaction volume was 25 ul, which contained 1X SYBR Green PCR buffer, 3 mM $MgCl_2$, 2.5 mM for each of the following nucleotide acids (dATP, dCTP, dGTP, 5mM dUTP), 0.025U/ul AmpliTaq Gold DNA polymerase, 0.01U/ul AmpErase UNG, 1.3 ul cDNA template, and 200 nM of oligonucleotide primer. The initial step of the PCR was a 10 minute hold at 95^0C followed by 45 cycles of the PCR amplification (95^0C 30 seconds, 60^0C 30 seconds, 72^0C 1 minute). For each experimental sample, the amount of target gene expression (*mPer1, mPer2 and Bmal1*) and housekeeping gene expression (S16 ribosomal protein gene) was determined based upon the threshold cycle. The content of the target gene expression was evaluated with respect to that of the housekeeping gene in each sample and expressed as the ratio of the target gene to reference gene. Every tumor and liver sample was tested in triplicate. Multiple no-template controls were included in all sets of the PCR amplification to test for the possible contamination of PCR reagents.

Statistical analysis

For each numerical value, such as the number of tumor mitotic figures, blood vessels, tumor sizes, growth rates, the mean and standard errors were calculated and graphed. Comparison of means across six circadian times of day (HALO) was assessed by one-way ANOVA (Super ANOVA, Abacus Corp, Berkeley, CA; SPSS, SPSS Inc, Chicago, Ill). Correlation analyses were done by the simple linear regressions. Pearson correlation coefficients were calculated. Numerical values from tumor and liver tissues as a function of different circadian times were also assessed for recurrent sinusoidal patterns and harmonics by Cosinor analysis with cosine curve-fitting tests using period fits of 12 hr, 24 hr and 12 plus 24 hr (Chronolab v4.5, Bioengineering & Chronobiology Laboratory, Pontevedra, Spain) and the best curve fitting results were chosen. Statistical significance was considered achieved if the zero amplitude hypothesis could be rejected at the 0.05 levels. All the data based upon the six circadian time periods were graphed as a double plot over 48 hours with standard errors of the means, as is customarily done to more easily visualize recurrent rhythmic patterns.

Results

Circadian Locomotor Cycle of Normal and Tumor Bearing Mice

Voluntary wheel running locomotor activity was measured before and after MTP tumor inoculation by continually recording wheel running activities of individual mice. Normal mice, prior to tumor cell inoculation, took 7-8 days to establish a stable daily running pattern. The locomotor activities of tumor bearing mice were maintained at normal levels with clear maintenance of circadian rhythmic pattern throughout the observation span (**Figure 2**). Mice with early tumors (day 10-13, linear growth stage) and those with later stage tumors (day 17-20) each showed normal circadian activity patterns with no differences in calculated 24 hour circadian period under LD schedule, 24 hour mean activity levels or activity during usual diurnal sleep span (measure of disturbance) when contrasted to their own individual and group wheel-running data during the week-long span just prior to tumor inoculation.

Daily Tumor Growth

Since the circadian locomotor rhythms of tumor bearing mice remain largely intact, we asked if tumor growth in these mice also displays circadian coordination. Three groups of mice had tumor measured daily at 12 hours intervals at six different

circadian times of day between days 10 and 13 post tumor cell inoculation. For group 1 mice in two separated experiments (**Figure 3a, b),** large consistent differences were seen in tumor growth rates at 8 HALO and 20 HALO circadian midpoints. When the tumor growth rates from these 12 hour intervals from each mouse in all 3 groups of mice were examined jointly, a clear circadian pattern of tumor growth is demonstrated (**Figure 3c**). Two peaks in tumor growth occur within each day. The higher daily peak occurs in late activity phase (18 HALO) and the second peak occurs each day in early sleep phase (6 HALO). These time-of-day

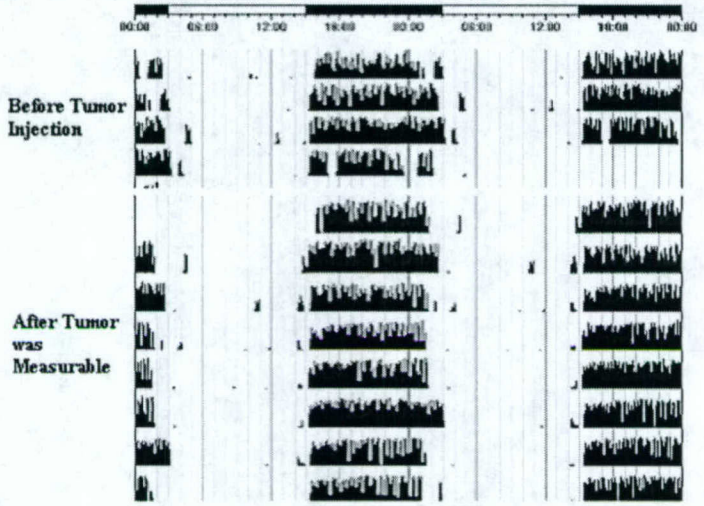

	Before Tumor	Days After Tumor		
		Day 10-13	Day 14-17	P-value
24 hr mean activity	18.3 +/- 5.5	20.0 +/- 5.5	22.2+/- 6.0	0.88
Activityduring sleep	1.5 +/- 2.1	2.1 +/- 2.9	2.0 +/- 3.0	0.81
Period*	24.3 +/- 0.7	24.4 +/- 0.7	24.2 +/- 0.5	0.74
Tumor size (mm^3)	NA	193 – 838	838 - 2238	

*Period analysis for LD schedule. P-value from ANOVA.

Figure 2. Circadian locomotor activity rhythms of mice before and after tumor injection. The voluntary locomotor activities of mice were recorded by wheel running for two weeks before tumor injection, during early (day 10-13) and later (day 14-17) tumor growth stages. Shown is the activity of one tumor-bearing mouse over successive days, double plotted. The mouse was regularly active in the dark (activity phase) and inactive in the light (sleep phase) both before and after tumor inoculation. The 24 mean activity, circadian period, and the amount of activity during sleep (disturbances) did not differ significantly between mice prior to tumor and mice with either early or late tumors.

differences in tumor size and growth rate are statistically significant by both ANOVA (p=0.0001) and Cosinor analyses (simultaneous 24 +12 hr period fit, p<0.001).

Daily Changes in Blood Vessels

It has been reported that daily tumor blood flow varies 1.5 fold, measured at two times of day, in rat tumor models with higher blood flow occurring during the mid dark/activity phase and lower flow at mid light/sleep phase(34). We determined whether the circadian variations of tumor growth were associated with rhythmic changes in tumor blood vessel density. PECAM protein immunohistochemical staining (CD31) is a typical marker for blood vessels and highlighted the vascular endothelial cells and tumor blood vessels clearly(35, 36). Tumor blood vessel density at 2, 6, 10, 14, 18, and 22 HALO was 8.6±2.2, 4.0± 0.9, 6.6 ± 1.4, 9.4±1.7, 8.6±1.9, and 8.2±2.3, respectively. Across all 6 times of day, these differences are not significantly different (ANOVA p=0.38, Cosinor, p=0.221). However, comparing just mid sleep/light (6 HALO) with mid activity/dark phase (18 HALO), statistically higher blood vessel density is found in mid activity (t-test, p=0.049), consistent with previous findings of higher tumor blood flow during the activity phase.

Tumor Cell Division

To determine whether the circadian variation of tumor growth was associated with circadian coordination of tumor cell proliferation, we quantified tumor cell mitosis in these same tumors. Large daily changes in tumor mitotic index were seen with a major (~3-fold) peak in late dark phase (22:20 HALO, late activity) and a second daily peak (11:20 HALO, late sleep) (ANOVA p=0.0012, Cosinor simultaneous 24 and 12 hour period fit p<0.001, **Figure 4a, 4b**).

Tumor Cell DNA Synthesis

Cyclin E protein, which is required for the initiation of DNA replication and subsequent mitosis(37-39), increases periodically in the late G_1 phase of the cell cycle(38). Cyclin E protein staining is seen primarily within the tumor cell nuclei (**Figure 4c**). Cyclin E expression varied rhythmically

throughout each day with 2.5 fold differences (**Figure 4d**). Two daily peaks in tumor cell cyclin E protein expression are present. A major peak occurs each day in the late dark/activity phase (21:20 HALO), just following the largest daily peak in tumor growth and just prior to the largest daily peak in mitosis, and another smaller peak in cyclin E occurs each day in late light/rest phase (9:20 HALO) (ANOVA p=0.0309, Cosinor simultaneous 24 plus 12 hour period fit p=0.006). The rhythm in tumor cell cyclin E protein expression tightly parallels the circadian rhythm of tumor size/growth (**Table 1**). Tumor cyclin E protein expression, which just precedes the daily mitotic peaks, also correlates with tumor cell mitotic index (r=0.337, p=0.02).

Rhythmic Expression of Circadian Clock Genes in Tumor and Liver Tissue

Tumor cell DNA synthesis and cell division are both gated within each day. Therefore, it is logical to ask whether clock gene expression is coordinating this cell cycle progression in normal tissues and cancer cells. We evaluated whether core clock gene expression is

(a)

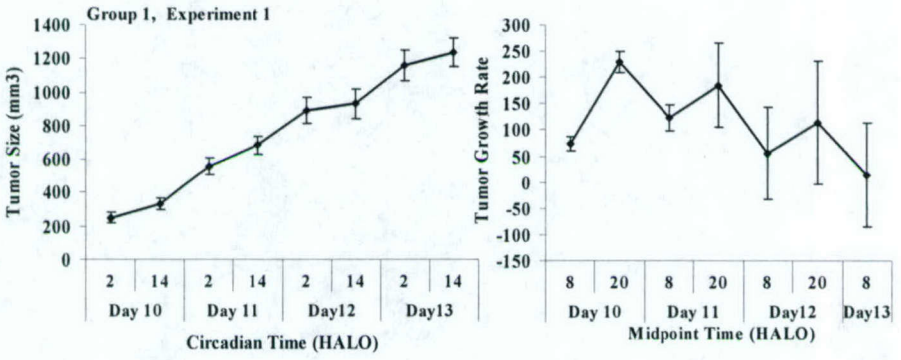

(b)

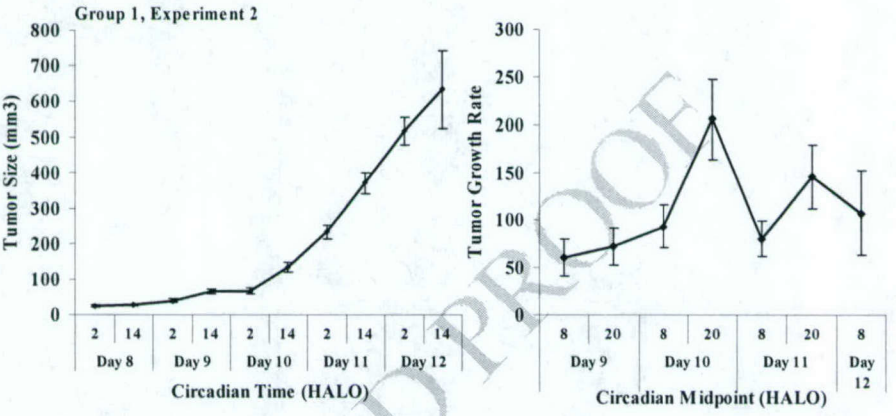

(c)

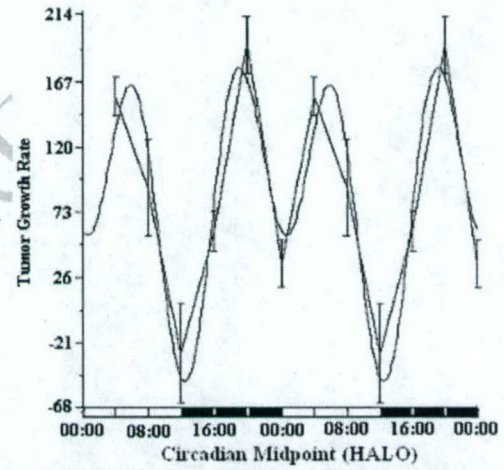

Figure 3. Tumor growth rates for all 12 hour time intervals during early tumor growth phase (day 10-13 in experiment 1, and day 8-12 in experiment 2, linear phase) are represented at the circadian midpoint between 12 hour measurements for each group of mice. Clear waxing and waning of change in tumor sizes or growth rates at different circadian intervals is evident. Figure 3a shows the tumor growth pattern of group 1 tumors in experiment 1. This

study design was reproduced in the experiment 2, with consistent waxing and waning in tumor size changes seen (Figure 3b). Circadian tumor growth rates from six circadian times are combined and represented at the six circadian midpoints between 12 hour measurements (Figure 3c). Tumor growth rates vary significantly throughout the day with two peaks per 24 hours; one slightly smaller peak at 6:30 HALO and another larger peak at 18:30 HALO (Cosinor 24hr plus 12 hr period fit, $p<0.001$).

coordinated throughout the day in these mouse tumors and within the histopathologically tumor free livers from these same tumor bearing mice. Previous studies in normal mice have described clock gene rhythms in liver (10, 11). Since sex hormonal milieu of female mice may affect host circadian gene expression(40), we avoided possible interference of the mouse's estrous cycle by analyzing clock gene expression only from tumors dissected from mice which were in the diestrus stage of the estrous cycle. Thirty-one pairs of tumor and liver tissues (5-6 pairs for each time of day) were analyzed for the expression of *Bmal1, mPer1, and*

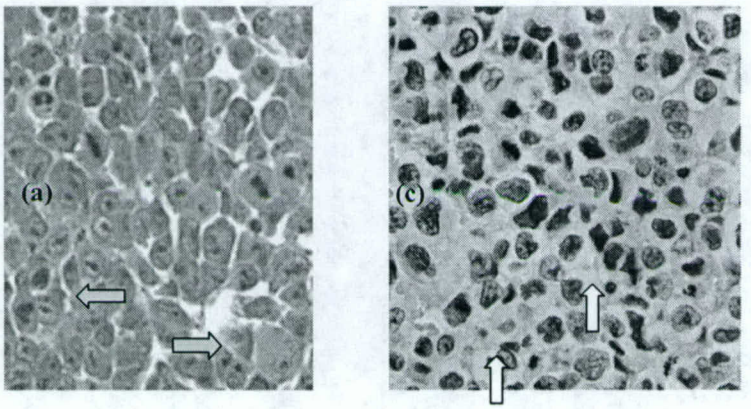

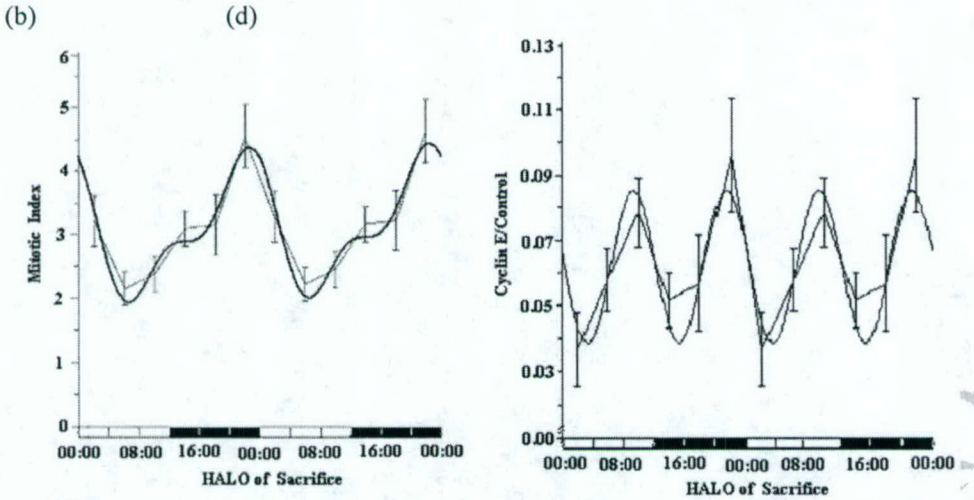

Figure 4. Mitotic figures (Figure 4a, x40 objective) of each tumor from mice sacrificed at specific times of day (HALO) were counted. The mitotic index (mitotic figures/high power field) of tumors (Figure 4b) shows a significant daily rhythm with two peaks each 24 hr cycle at 11:20 (minor peak) and 22:20 (major peak) HALO (Cosinor 24 hr plus 12 hour period fit, $p<0.001$). Tumor cyclin E protein staining is mainly seen in the nucleus of tumor cells (Figure 4c, x40 objective). Cyclin E protein expression showed a daily rhythmic pattern (Figure 4d) with two peaks per 24 hr cycle; one at 9:20 and another at 21:20 HALO (Cosinor 12 hr period fit, $p=0.006$).

mPer2. A circadian rhythm was seen in liver *mPer1, mPer2 and Bmal1* (**Figure 5a-c**, all $p< 0.001$). Liver clock gene expression peaks at 11:20 HALO for *mPer2,* 21:00 HALO for *Bmal1,* and a major peak in *mPer1* at 7:10 HALO. However, *mPer1* expression, in contrast to *mPer2* and *Bmal1*, displays two peaks per day, one major at 7:10 HALO (midsleep) and a second minor peak at 19:10 HALO (midactivity) (**Figure 5b**, Cosinor 24 hours plus 12 hour period fit, $p<0.001$). This twice daily or 12 hour pattern in *mPer1* gene expression is identical to the pattern we previously reported in *hPer1* in human skin and oral mucosa(24). These circadian gene expression patterns in the livers from our tumor bearing mice are very similar in magnitude and timing to those reported in livers from non-tumor bearing mice(41-45). In this MTP mammary tumor, *mPer1 and mPer2* gene expression was present, but, no statistically significant time of day differences were seen (**Figure 5a, b**). However, *Bmal1* expression in these tumors varies significantly throughout the day (**Figure 5d**, $p=0.022$). The circadian pattern of the tumor *Bmal1* gene expression is very similar to *Bmal1* daily rhythm

in host liver, both showing a peak in expression at around 21:00 HALO and a trough at around 9:00 HALO. The daily fold difference of *Bmal1* expression in liver, however, was 26.1 fold, while that in tumors is 2.1 fold.

In summary, tumor bearing mice, in normal diurnal conditions, are circadian entrained, as reflected by the normal host locomotor activity rhythms and rhythmic liver clock gene expression (**Table 1, Figure 6).** The tumors within these mice are also circadian organized, as reflected by circadian coordination of tumor growth, tumor DNA synthesis (cyclin E), tumor cell mitosis, and circadian clock gene expression (*Bmal1*), but with an apparent loss of rhythmic expression of other clock genes (*mPer1 and mPer2*). Daily peaks in tumor cell growth rates are immediately followed in time by peaks in tumor cell cyclin E. Daily peaks in tumor cell mitosis occur at times removed from those of growth and DNA synthesis, and the major peak in mitosis follows that in *Bmal1* expression.

Table 1. Circadian Organization of Tumor Bearing Mice and their Malignant and Normal Tissues.

		Daily Rhythm	P-value (Cosinor)	Peaks /24 hrs	Peak time (HALO)[a]	Daily Changes (min ; max)	Daily Fold Differences (max/min)
Locomotor Activity	Tumor Bearing Mouse	Yes	<0.001	1	18:50	0.10 ; 874.0	8700
Tumor Growth Rate		Yes	< 0.001	2	06:50 19:20	-68.0 ; 214.0	-[b]
Tumor Cell Cycle							
Cyclin E	Tumor	Yes	0.006	2	09:20 21:20	0.045 ; 0.115	2.5
Mitosis	Tumor	Yes	<0.001	2	11:20 22:20	1.80 ; 5.30	2.9
Clock Genes							
Bmal 1	Liver	Yes	<0.001	1	21:00	1.50 ; 40.00	26.7
	Tumor	Yes	0.022	1	21:40	0.87 ; 1.87	2.1
mPer 1	Liver	Yes	<0.001	2	07:10 19:10	0.85 ; 2.85	3.4
	Tumor	No	0.54	-	-	-	-
mPer 2	Liver	Yes	<0.001	1	11:20	0.80 ; 6.95	8.7
	Tumor	No	0.29	-	-	-	-

[a]HALO=Hours After Light onset in 12L/12D 24-hour cycle.

[b]Not available due to the negative value.

Discussion

Circadian Coordination of the Cancer Host Interrelationship

The balance between the host and cancer have been shown to participate powerfully in biological rhythms(26). The difference between cancer patient death and cure can depend upon the timing of therapy within the daily or menstrual cycles of cancer patients(20, 30). The central circadian pacemaker in the SCN coordinates host circadian rhythms i.e. the daily sleep/activity cycle, the circadian order of hormone production, and even the dynamics of cell cycle traverse (21). The environment and daily behavior patterns (light, food intake, behavior) reset these rhythms each day. Cancer-bearing mice and patients maintain their circadian organization, to some extent, during early stages of cancer growth. These circadian rhythmicities are often altered, but seldom, if ever, abolished later in the course of cancer progression. Severe alterations of host circadian organization are usually associated with poor prognosis and death (46, 47).

This is the first time that the circadian pattern of cancer growth, cancer cell proliferation, and cancer cell core clock gene expression have been concurrently measured. In this study, we have monitored the circadian locomotor cycle of tumor bearing mice from the day of tumor cell inoculation to late stage of tumor growth. The daily putative sleep/activity rhythms of these mice are identical (period, activity level, sleep disturbances) to those of normal non-tumor bearing mice, indicating that the environmentally synchronized host circadian clocks remain organized within these mice with growing, local, non-metastatic tumors. In the tumor-free host liver tissue from these mice, circadian rhythms in clock gene expression (*mPer1, mPer2, Bmal1)* remain coordinated and are similar in amplitude and phase to those reported in non-tumor bearing mice(41-45).

Circadian Coordination of Tumor Growth and Cell Cycle Events

Hori* et al *is the first to have shown faster microscopic tumor growth and higher blood flow in tumors observed microscopically, twice daily, during mid dark/activity compared to mid light/sleep(48, 49). We demonstrate, for the first time in non-instrumented animals, that gross tumor growth rate waxes and wanes, unsubtly, during each day if tumor size is simply measured 6 times round the clock. Two daily peaks in cancer growth rate occur each day. The fastest tumor growth occurs during mid-activity and second peak occurs during mid-sleep. These findings are consistent with Hori's results(48). The time of day changes in tumor growth which we observed are explained only in part by differences in tumor blood vessel density, and more fully by ordered daily pulses of both tumor cell DNA-synthesis and tumor cell division.

Scheving *et al* were the first to report a significant circadian rhythm of mitotic activity in human epidermis(12). We described the circadian coordination of cancer cell mitotic index in a human skin cancer(26) which is consistent with several previous clinical studies showing time of day differences in human cancer biology(50, 51). Similar circadian rhythmic coordination in mitotic index and S phase tumor cell distribution has also been reported in rodent tumor models(52, 53). We evaluated the tumor cell circadian rhythms of tumor cell mitosis and DNA synthesis/cyclin E cell cycle checkpoint protein in the same tumors in which tumor growth rate differences were concurrently measured, round the clock. We also concurrently

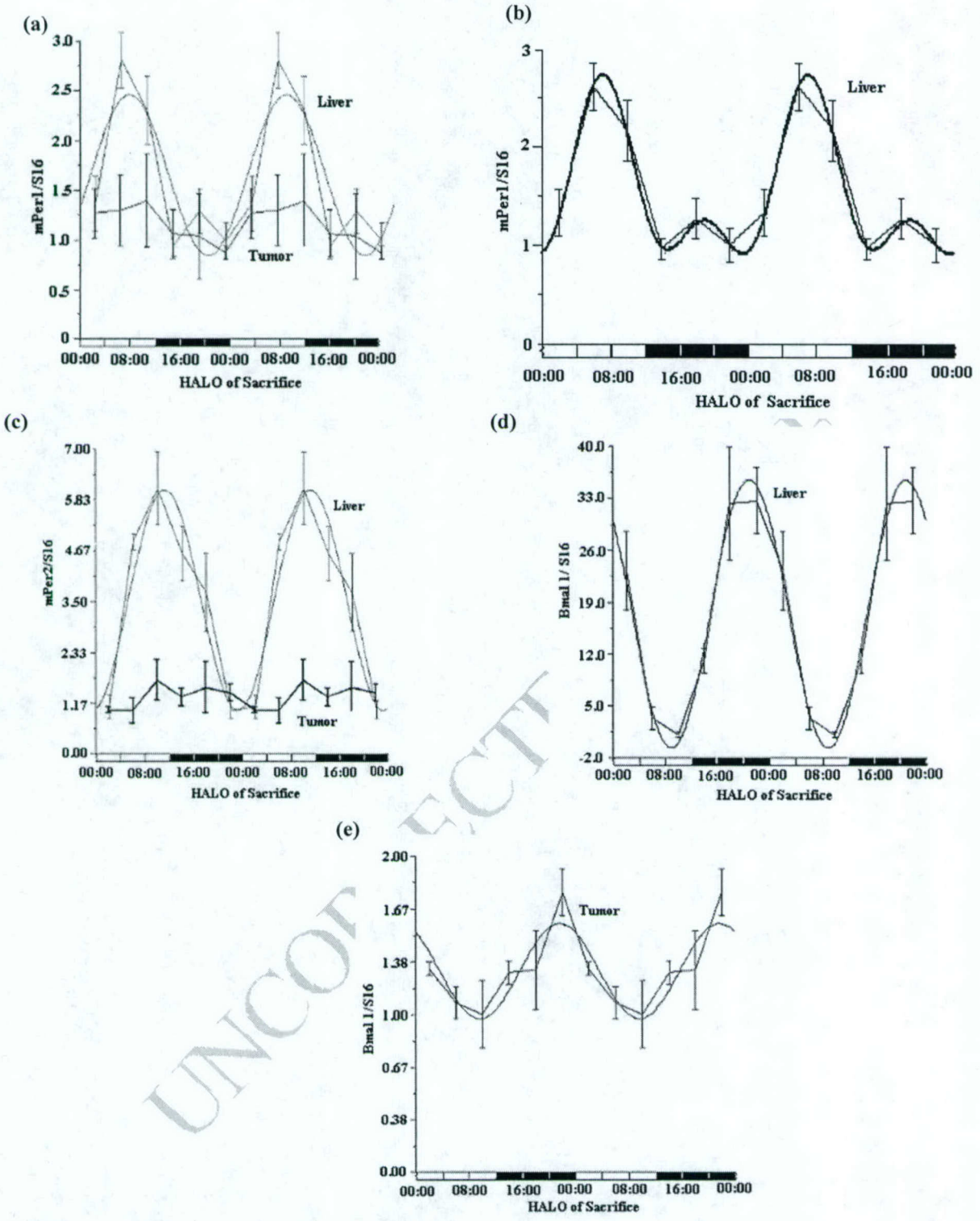

Figure 5. *mPer 1* and *mPer 2* mRNA expression (as ratio to S16 control gene) in paired mouse mammary tumor and liver tissues from tumor bearing mice in early tumor stages. Significant daily rhythmic patterns of *mPer 1* and *mPer 2* gene expression were seen in the livers of tumor bearing mice with major peak times at 7:10 HALO and 11:20 HALO, respectively (Cosinor 24 hr curve fit, $p_{mPer\ 1} < 0.001$, $p_{mPer\ 2} < 0.001$). Daily rhythms were not detectable in *mPer 1* and *mPer 2* in tumors from these same mice ($p_{mPer1} = 0.54$, $p_{mPer2} = 0.56$) (a) and (c). *mPer1* in liver best fits a 24 plus 12 hour rhythm with a major peak at 7:10 and a minor peak at 19:10 HALO (b). A significant daily rhythm of *Bmal-1* gene expression was demonstrated in the paired tumor and liver tissues, respectively ($p_{tumor} = 0.022$, $p_{liver} < 0.001$). By 24 hr Cosinor period fit, liver and tumor, showed one daily peak in *Bmal-1* expression at 21:00 and 21:40 HALO, respectively. However, the amplitude of the tumor *Bmal-1* is much lower than that seen in the liver (d) and (e).

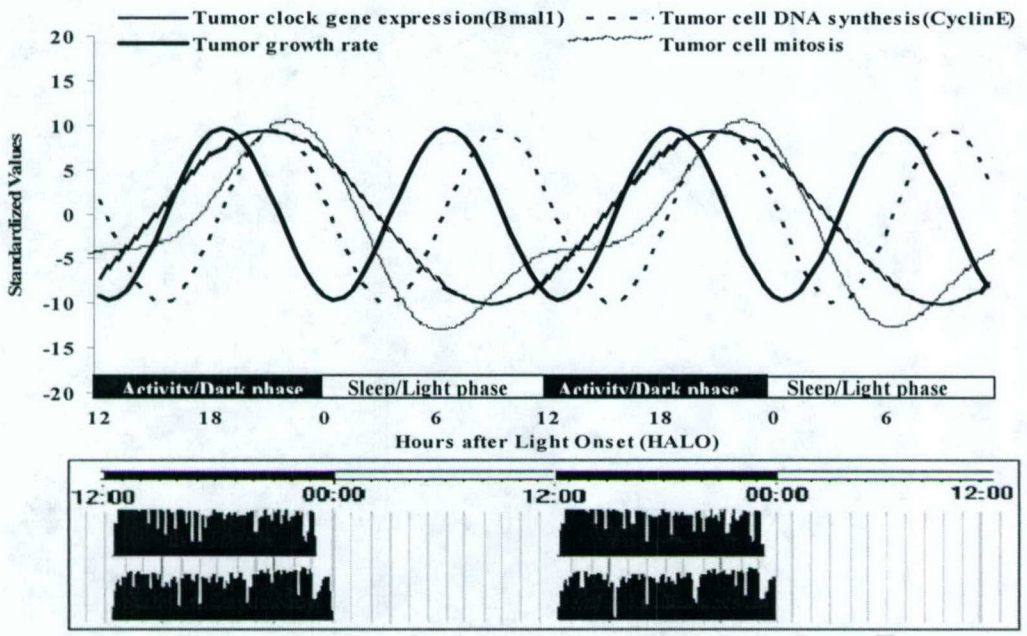

Figure 6. Daily sequencing of tumor cell cycle events, tumor growth, tumor clock gene expression and host locomotor activity. Shown are the standardized fitted curves in tumor cell DNA synthesis, tumor cell mitosis, and tumor growth, which coordinately wax and wane within a day and may be putatively linked to tumor peripheral clock (*Bmal1*) gene expression and host's sleep/activity cycle. Peaks in tumor cell growth rate are immediately followed in time by peaks in tumor cyclin E protein. Peaks in tumor cell growth occur at times removed from those of DNA synthesis and mitosis, and the major peak in mitosis just follows that in *Bmal1*.

measured circadian clock gene expression. Both the G1/S checkpoint protein (cyclin E) expression and tumor cell mitotic index vary rhythmically along a 24 hour span with 2-3 fold daily differences in a largely overlapping pattern with the rhythm in tumor growth rate, suggesting that the same oscillator or pacemaker, may be controlling each of these rhythms. These observations obviously reflect the daily population dynamic of cell cycle traverse in the tumor. Resolution of what is happening at the single cell level requires determination of individual cell dynamics and requires serial non-destructive cellular observation *in vivo,* such as functional nuclear magnetic resonance and concurrent pathway specific molecular emission techniques.

Circadian Coordination of Clock Gene Expression

***The expression of the three key core clock genes remains highly rhythmic in the liver cells from tumor bearing mice. These findings are consistent with the retention of normal circadian patterns of locomotor activity in these tumor bearing mice. In the tumor cells from these same mice,* Bmal1 *mRNA is rhythmically expressed throughout the day with the same timing of the peak expression as that of the host liver, but with a much lower daily amplitude. The expected tumor circadian rhythm in* mPer1 *and* mPer2 *has, however, been lost. These analyses of tumor clock gene expression were performed on bulk tumor tissue, which is heterogeneous, with areas of necrosis and host stromal cells(31). Further studies will employ microdissection to diminish sampled tumor tissue heterogeneity by selecting only "healthy" tumor cells for gene expression analysis. Daily changes in* mPer1 *and* mPer2 *protein levels will also need to be determined in these tumors. Given the data that we have, however, we must tentatively conclude that these tumor cells have partially lost their responsiveness to the host's circadian system. If these tumor cells have, in fact, lost their circadian coordination of* mPer1 *and* mPer2*, it is clear that they have not lost the circadian organization of tumor growth, DNA synthesis or mitosis. This may mean that circadian clock function is redundant.* Bmal1 *expression, with or without the coordination of other core clock genes, which we have not yet measured, may be adequate to transmit the circadian information essential to coordinate daily fundamental cancer cellular biology and to link these tumor cell proliferations to the central circadian clock. These data show that circadian organization in cancer cells persists without fully normal peripheral core clock gene expression. This raises therapeutic*

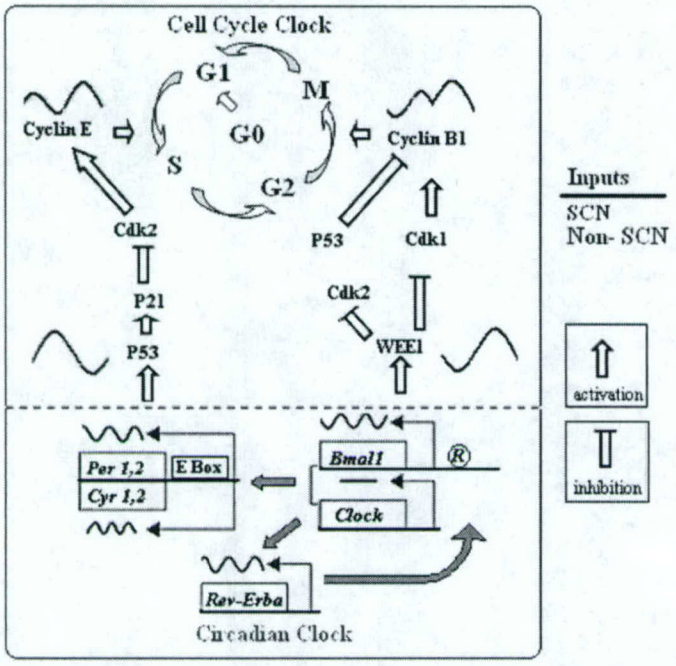

Figure 7. Proposed coordination between cell cycle progression and peripheral circadian clocks. The clock gene products construct precisely timed feedback loops within peripheral tissues, which are normally entrained by the same circadian clock in the SCN, as well as by rhythmic inputs from non-SCN inputs (e.g. feeding). Tissue peripheral clock gene products may be functional modulators of the cell cycle. For example, *Bmal1* expression, which peaks during the late dark phase of a day, activates the expression of *Wee1*, and *Wee1* phosphorylates Cdk 1 and Cdk 2, and inactivates these kinases. Consequently, both cyclin E and B1 are activated and promote the cell cycle transition from G1 to S and from G2 to M, which may coordinate the peaks of cyclin E (DNA synthesis) and mitosis during the late dark phase of the day. *Per1* expression peaks during the mid light phase of a day and up regulates P53 protein expression, which subsequently down regulates cyclin B1 expression and stimulates the expression of P21 protein. Down regulation of cyclin B1 directly inhibits cell mitosis while accumulation of P21 protein inhibits Cdk2 and stimulates cyclin E, which may coordinate the peak of cyclin E (DNA synthesis) during the mid light phase of the day. The daily rhythm in *Per1* gene expression (and *Per2*), however, may not be critical since it was absent in these tumors which still maintained these rhythms in cell cycle events. E box response elements (or other response elements, R) are common to clock genes and cell cycle genes.

cancer cells might help to control their growth. A third possibility must also be entertained, namely that circadian core clock gene expression within cancer cells is irrelevant to the demonstrated circadian coordination of cancer cell proliferation and cancer growth.

How are circadian clock genes linked to cellular proliferation?

Cell cycle traverse is mediated by a number of cellular proteins. Cyclin E, which binds to Cdk2, shows peak of expression in late G_1(54) Cyclin E-Cdk2 activity is required for initiation of DNA replication and for transition from G_1 to S phase(39). Cyclin B1 is a key regulator of the transition of cells from G_2 to M phase. Cdk1 forms an inactive heterodimeric complex with cyclin B1 which is maintained in an inactive form by phosphorylation by WEE1 kinase(54). Cdk1 is converted to an active form by dephosphorylation by the dual specificity phosphatase, Cdc25C(55). P21, as well as WEE1, each modulate the activities of a number of Cdks acting as multi-potential Cdk inhibitors causing cell cycle arrest at either G_1/S or G_2/M interfaces(56-58). P53 functions in controlling the G_1/S and G_2/M transitions by increasing the level of P21 protein and by decreasing expression level of cyclin B1(59). Matsuo *et al.* showed that the circadian clock coordinated the expression of cell cycle-related genes, such as *wee1*, which in turn modulated the timed expression of active Cyclin B1-Cdc2 kinase (Cdk1) (60). Fu *et al.* showed that several cell cycle regulated proteins (e.g. Cyclin D_1, Cyclin A, mdm-2, and gadd45α) were circadian disorganized in *Per2* mutant mice(61). Bjarnason *et al.* reported the ordered expression of P53, cyclin E, cyclin A, cyclin B1, and Ki 67 proteins throughout the day in normal oral mucosal biopsies (24, 62). The rhythmicity of cell mitosis was coordinated with the rhythmicity of *Bmal1* gene expression both in normal human oral mucosa and in our mammary tumors (24, 63). The use of E-box DNA response elements, common to both circadian clock genes(64) and cell cycle genes(65), may allow for coordination between circadian clocks and cell cycle (Figure 7).

In summary, these data are the first to show that daily rhythms in cancer growth, cancer cell DNA synthesis, cancer cell mitosis and at least one cancer clock gene expression pattern are each maintained within cancer cells *in vivo*. They further show that coordinate circadian expression of all circadian clock genes may not be essential for the daily coordination of cancer cell proliferation, indicating that circadian controls of fundamental cellular processes may well be either both robust and redundant or irrelevant. These data mean that the timing of any drug targeting a cancer cell proliferation-related target if given at optimal times within the day, may improve therapeutic effects.

Acknowledgements

We thank Dr. Bernard Fisher for providing the C3H/MTP mammary tumor. We thank summer students who attended in this work, S. Bickley, B. Nassri, X. You, and C. Hrushesky. This work is supported by VA merit award (Hrushesky W), **Department of Defense breast cancer research fund DAMD17-98-1-8016 (Hrushesky W),** VA VISN 7 career development award (You S), VA merit award (Wood P), and Mochida Memorial Foundation for Medical and Pharmaceutical Research (Kobayashi M).

References:

1. Pittendrigh CS. Temporal organization: reflections of a Darwinian clock-watcher. Ann Rev Physiol 1993;55:16-54.
2. Vitaterna MH, King DP, Chang AM, Kornhauser JM, Lowrey PL, McDonald JD, et al. Mutagenesis and mapping of a mouse gene, clock, essential for circadian behavior. Science 1994;264:719-725.
3. King DP, Zhao Y, Sangoram AM, Wilsbacher LD, Tanaka M, Antoch MP, et al. Positional cloning of the mouse circadian clock gene. Cell 1997;89(4):641-53.
4. Tei H, Okamura H, Shigeyoshi Y, Fukuhara C, Ozawa R, Hirose M, et al. Circadian oscillation of a mammalian homologue of the Drosophila period gene. Nature 1997;389(6650):512-6.
5. Sun ZS, Albrecht U, Zhuchenko O, Bailey J, Eichele G, Lee CC. RIGUI, a putative mammalian ortholog of the Drosophila period gene. Cell 1997;90(6):1003-11.
6. Gekakis N, Staknis D, Nguyen HB, Davis FC, Wilsbacher LD, King DP, et al. Role of the CLOCK protein in the mammalian circadian mechanism. Science 1998;280(5369):1564-9.
7. Sangoram AM, Saez L, Antoch MP, Gekakis N, Staknis D, Whiteley A, et al. Mammalian circadian autoregulatory loop: a timeless ortholog and mPer1 interact and negatively regulate CLOCK-BMAL1-induced transcription. Neuron 1998;21(5):1101-13.
8. Davidson AJ, Poole AS, Yamazaki S, Menaker M. Is the food-entrainable circadian oscillator in the digestive system? Genes Brain Behav 2003;2(1):32-9.
9. Stokkan KA, Yamazaki S, Tei H, Sakaki Y, Menaker M. Entrainment of the circadian clock in the liver by feeding. Science 2001;291(5503):490-3.
10. Zylka MJ, Shearman LP, Weaver DR, Reppert SM. Three period homologs in mammals: differential light responses in the suprachiasmatic circadian clock and oscillating transcripts outside of brain. Neuron 1998;20(6):1103-10.
11. Sakamoto K, Nagase T, Fukui H, Horikawa K, Okada T, Tanaka H, et al. Multitissue circadian expression of rat period homolog (rPer2) mRNA is governed by the mammalian circadian clock, the suprachiasmatic nucleus in the brain. J Biol Chem 1998;273:27039-27042.
12. Scheving LE. Mitotic activity in the human epidermis. Anat Rec 1959;135:7-19.

13. Smaaland R, Laerum O, Lote K, Sletvold O, Sothern R, Bjerknes R. DNA synthesis in human bone marrow is circadian stage dependent. Blood 1991;77:2603-2611.
14. Buchi K, Moore J, Hrushesky W, Sothern R, Rubin N. Circadian rhythm of cellular proliferation in the human rectal mucosa. Gastroenterology 1991;101:410-415.
15. Scheving LE, Burns ER, Pauly JE, Halberg F, Haus E. Survival and cure of leukemic mice after circadian optimization of treatment with cyclophosphamide and 1-beta-D-arabinofuranosylcytosine. Cancer Res 1977;37(10):3648-55.
16. Haus E, Halberg F, Scheving L, Cardoso S, Kuhl JFW, Sothern R, et al. Increased tolerance of mice to arabinosylcytosine given on schedule adjusted to circadian system. Science 1972;177:80-82.
17. Hrushesky WJ, Bjarnason GA. Circadian cancer therapy. J Clin Oncol 1993;11(7):1403-17.
18. Hrushesky WJ. Circadian timing of cancer chemotherapy. Science 1985;228(4695):73-5.
19. Lévi F, Zidani R, Misset J-L. Randomised multicentre trial of chronotherapy with oxaliplatin, fluorouracil, and folinic acid in metastatic colorectal cancer. Lancet 1997;360:681-86.
20. Levi FA, Zidani R, Vannetzel JM, Perpoint B, Focan C, Faggiuolo R, et al. Chronomodulated versus fixed-infusion-rate delivery of ambulatory chemotherapy with oxaliplatin, fluorouracil, and folinic acid (leucovorin) in patients with colorectal cancer metastases: a randomized multi-institutional trial. J Natl Cancer Inst 1994;86(21):1608-17.
21. Wood PA, Hrushesky WJ. Circadian rhythms and cancer chemotherapy. Crit Rev Eukaryot Gene Expr 1996;6(4):299-343.
22. Wood PA, Hrushesky WJ, Klevecz R. Distinct circadian time structures characterize myeloid and erythroid progenitor and multipotential cell clonogenicity as well as marrow precursor proliferation dynamics. Exp Hematol 1998;26(6):523-33.
23. Lincoln D, Hrushesky W, Wood P. Circadian organization of thymidylate synthase activity in normal tissues: a possible basis for 5-fluorouracil chronotherapeutic advantage. Int J Cancer 2000;88:479-485.
24. Bjarnason G, Jordan R, Wood P, Li Q, Lincoln D, Sothern R, et al. Circadian expression of clock genes in human oral mucosa and skin: association with specific cell cycle phases. Am J Pathol 2001;158:1793-1801.
25. Sothern RB, Levi F, Haus E, Halberg F, Hrushesky WJM. Control of a murine plasmacytoma with doxorubicin-cisplatin: dependence on circadian stage of treatment. J Natl Cancer Inst 1989;81(2):135-145.
26. Hrushesky WJ, Lannin D, Haus E. Evidence for an ontogenetic basis for circadian coordination of cancer cell proliferation. J Natl Cancer Inst 1998;90(19):1480-4.
27. Smaaland R, Lote K, Sothern RB, Laerum OD. DNA synthesis and ploidy in non-Hodgkin's lymphomas demonstrate intrapatient variation depending on circadian stage of cell sampling. Cancer Res 1993;53:3129-3138.
28. Klevecz RR, Shymko RM, Blumenfeld D, Braly PS. Circadian gating of S phase in human ovarian cancer. Cancer Res 1987;47:6267-6271.
29. Fisher B, Fisher, E. Experimental evidence in support of the dormant tumor cell Science. Science 1959;130:918-919.
30. Hrushesky WJM, Bluming AZ, Gruber SA, Sothern RB. Menstrual influence on surgical cure of breast cancer. Lancet 1989;ii:949-952.
31. You S, Li W, Kobayashi M, Xiong Y, Hrushesky WJ, Wood PA. Creation of a stable mammary tumor cell line that maintains fertility cycle tumor biology of the parent tumor. In Vitro Cell Dev Biol Anim 2004;40(3 in press).
32. Wells W, Rainer, RO., Memoli, VA. Basic principles of image processing. Am J Clin Pathol. 1992;98:493-501.
33. You S, Yao, K., Cao, Y. Latency of Epstein-Barr virus and its relationship to nasopharyngeal carcinomas. Zhonghua Zhong Liu Za Zhi. 1996;18:23-26.
34. Hori K, Zhang QH, Li HC, Saito S. Variation of growth rate of a rat tumour during a light-dark cycle: correlation with circadian fluctuations in tumour blood flow. Br J Cancer 1995;71(6):1163-8.
35. Bevilacqua P, Barbareschi, M., Verderio P., Boracchi, P., Caffo, O., Dalla Palma, P., Meli, S., Weidner, N., Gasparini, G. Prognostic value of intratumoral microvessel density, a measure of tumor angiogenesis, in node-negative breast carcinoma--results of a multiparametric study. Breast Cancer Res Treat. 1995;36:205-217.
36. Laforga J, Aranda, FI. Angiogenic Index: a new method for assessing microvascularity in breast carcinoma with possible prognostic implications. Breast J 2000;6:103-107.
37. Koff A, Giordano A, Desai D, Yamashita K, Harper JW, Elledge S, et al. Formation and activation of a cyclin E-cdk2 complex during the G1 phase of the human cell cycle. Science 1992;257(5077):1689-94.
38. Koff A, Cross F, Fisher A, Schumacher J, Leguellec K, Philippe M, et al. Human cyclin E, a new cyclin that interacts with two members of the CDC2 gene family. Cell 1991;66(6):1217-28.
39. Ohtsubo M, Theodoras AM, Schumacher J, Roberts JM, Pagano M. Human cyclin E, a nuclear protein essential for the G1-to-S phase transition. Mol Cell Biol 1995;15(5):2612-24.
40. Abizaid A, Mezei G, Horvath TL. Estradiol enhances light-induced expression of transcription factors in the SCN. Brain Res 2004;1010(1-2):35-44.
41. Hara R, Wan K, Wakamatsu H, Aida R, Moriya T, Akiyama M, et al. Restricted feeding entrains liver clock without participation of the suprachiasmatic nucleus. Genes Cells 2001;6(3):269-78.
42. Jin X, Shearman LP, Weaver DR, Zylka MJ, de Vries GJ, Reppert SM. A molecular mechanism regulating rhythmic output from the suprachiasmatic circadian clock. Cell 1999;96(1):57-68.
43. Lee C, Etchegaray JP, Cagampang FR, Loudon AS, Reppert SM. Posttranslational mechanisms regulate the mammalian circadian clock. Cell 2001;107(7):855-67.
44. Oishi K, Fukui H, Ishida N. Rhythmic expression of BMAL1 mRNA is altered in Clock mutant mice: differential regulation in the suprachiasmatic nucleus and peripheral tissues. Biochem Biophys Res Commun 2000;268(1):164-71.
45. Takata M, Burioka N, Ohdo S, Takane H, Terazono H, Miyata M, et al. Daily expression of mRNAs for the mammalian Clock genes Per2 and clock in mouse suprachiasmatic nuclei and liver and human peripheral blood mononuclear cells. Jpn J Pharmacol 2002;90(3):263-9.

46. Mormont M, De Prins J, Levi F. Study of circadian rhythm of activity by actometry: preliminary results in 30 patients with metastatic colorectal cancer. Path Biol 1996;3:165-171.
47. Sephton SE, Sapolsky RM, Kraemer HC, Spiegel D. Diurnal cortisol rhythm as a predictor of breast cancer survival. J Natl Cancer Inst 2000;92(12):994-1000.
48. Hori K, Zhang Q-H, Li H-C, Saito S. Variation of growth rate of a rat tumour during a light-dark cycle: correlation with circadian fluctuations in tumour blood flow. Br J of Cancer 1995;71:1163-1168.
49. Hori K, Suzuki M, Tanda S, Saito S, Shinozaki M, Zhang QH. Circadian variation of tumor blood flow in rat subcutaneous tumors and its alteration by angiotensin II-induced hypertension. Cancer Res 1992;52(4):912-6.
50. Voutilainen A. Über die 24-stunden-rhythmik der mitozfrequenz in malignen tumoren. Acta Path Microb Scan 1953;99(suppl.):1-104.
51. Tähti E. Studies of the effect of x-irradiation on 24 hour variations in the mitotic activity in human malignant tumours. Acta Path Microbiol Scand 1956;117:1-61.
52. Nash RE, Llanos JM. Twenty-four-hour variations in DNA synthesis of a fast-growing and a slow-growing hepatoma: DNA synthesis rhythm in hepatoma. J Natl Cancer Inst 1971;47(5):1007-12.
53. Burns E, Scheving L, Tsai T. Circadian rhythms in DNA synthesis and mitosis in normal mice and in mice bearing the Lewis lung carcinoma. Eur J Cancer 1979;15:233-242.
54. McGowan CH, Russell P. Cell cycle regulation of human WEE1. Embro J 1995;14(10):2166-75.
55. Jin P, Gu Y, Morgan DO. Role of inhibitory CDC2 phosphorylation in radiation-induced G2 arrest in human cells. J Cell Biol 1996;134(4):963-70.
56. Watanabe N, Broome M, Hunter T. Regulation of the human WEE1Hu CDK tyrosine 15-kinase during the cell cycle. Embro J 1995;14(9):1879-1891.
57. Sherr CJ, Roberts JM. Inhibitors of mammalian G1 cyclin-dependent kinases. Genes Dev 1995;9(10):1149-63.
58. Tchou WW, Rom WN, Tchou-Wong KM. Novel form of p21(WAF1/CIP1/SDI1) protein in phorbolester-induced G2/M arrest. J Biol Chem 1996;271(47):29556-60.
59. Badie C, Bourhis J, Sobczak-Thepot J, Haddada H, Chiron M, Janicot M, et al. p53-dependent G2 arrest associated with a decrease in cyclins A2 and B1 levels in a human carcinoma cell line. Br J Cancer 2000;82(3):642-50.
60. Matsuo T, Yamaguchi S, Mitsui S, Emi A, Shimoda F, Okamura H. Control mechanism of the circadian clock for timing of cell division in vivo. Science 2003;302(5643):255-9.
61. Fu L, Pelicano H, Liu J, Huang P, Lee CC. The circadian gene *period2* plays an important role in tumor suppression and DNA damage response in *vivo*. Cell 111 2002:41-50.
62. Bjarnason GA, Jordan RC, Sothern RB. Circadian variation in the expression of cell-cycle proteins in human oral epithelium. Am J Pathol 1999;154(2):613-22.
63. You S, Xiong Y, Kobayashi M, Wood P, Bickley S, Simu M, et al. Tumor cell circadian clock genes are rhythmically expressed in coordination with rhythmic circadian growth and thereby may represent new therapeutic targets. Clin. Cancer Res. 2003;9(16):6126s.
64. Darlington TK, Lyons LC, Hardin PE, Kay SA. The period E-box is sufficient to drive circadian oscillation of transcription in vivo. J Biol Rhythms 2000;15(6):462-71.
65. Farina A, Gaetano C, Crescenzi M, Puccini F, Manni I, Sacchi A, et al. The inhibition of cyclin B1 gene transcription in quiescent NIH3T3 cells is mediated by an E-box. Oncogene 1996;13(6):1287-96.

Address for offprints and correspondence: William JM Hrushesky, WJB Dorn Veterans Affairs Medical Center (151), 6439 Garners Ferry Road, Columbia, South Carolina 29209. Tel. 803-647-5654; Fax. 803-647-5656. Email: william.hrushesky@med.va.gov

In Vitro Cell. Dev. Biol.—Animal 40:000–000, April 2004

1071-2690/04 $18.00+0.00

CREATION OF A STABLE MAMMARY TUMOR CELL LINE THAT MAINTAINS FERTILITY-CYCLE TUMOR BIOLOGY OF THE PARENT TUMOR

SHAOJIN YOU, WEI LI, MINORU KOBAYASHI, YIN XIONG, WILLIAM HRUSHESKY, AND PATRICIA WOOD[1]

Dorn Research Institute, WJB Dorn Veterans Affairs Medical Center (151), 6439 Garners Ferry Road, Columbia, South Carolina 29209

(Received 26 March 2004; accepted 13 May 2004)

SUMMARY

A mammary tumor cell line, designated MTCL, was successfully established from a mouse primary mammary tumor (MTP). The MTCL cells retain cytokeratin and both estrogen receptor (ER) and progesterone receptor (PR) in vitro. In vitro exposure of MTCL cells to progesterone causes a decrease in the cellular ^{3}H-thymidine uptake, indicating an inhibition by progesterone on MTCL cellular deoxyribonucleic acid synthesis, whereas exposure of the cells to a high dose of estrogen (15 pg/ml) for 48 h causes an increase of ^{3}H-thymidine uptake. We inoculated both MTP or MTCL tumor cells into normal cycling female C_3HeB/FeJ mice and demonstrated that the post-resection metastatic recurrence of MTCL tumors, like the original MTP tumors, depends on the time of tumor resection within the mouse estrous-cycle stage. Both MTCL and MTP tumors have similar histological appearances with the exception of less extensive tumor necrosis and higher vascularity in MTCL tumors. Equivalent levels of sex hormone receptors (ER α, ER β, and PR), epithelial growth hormone receptors (Her2/neu, EGFR1), tumor suppressors (BRCA1, PS3), and cell apoptosis–relevant protein (bcl-xl) were found in these in vivo tumors by immunohistochemistry. Cyclin E protein, however, was significantly higher in MTP tumors compared with MTCL tumors. Our results indicate that MTCL cells retain many of the biologic features of the original MTP primary tumor cells, and to our knowledge, it is the first in vitro cell line that has been shown to maintain the estrous-cycle dependence of in vivo cancer metastasis.

Key words: mammary neoplasma; surgery; fertility cycle; metastasis.

INTRODUCTION

The cells of the human breast, as well as cancer cells arising within this organ, are profoundly affected by female sex hormones. Beatson (1896), more than 100 yr ago, demonstrated that removing the ovaries, which cyclically produce sex hormones (progesterone and estrogen), from young women with advanced breast cancer caused the cancer to shrink and in some cases disappear entirely. In the ensuing years, many of the biochemical and molecular connections between sex hormones and breast cancer progression have been better defined. Because of our interest in biologic rhythms, such as the estrous (in mice) or menstrual (in women) cycle, we did a series of tumor resection experiments in groups of cycling female mice (Ratajczak et al., 1988; Bove et al., 2002). We found that an operation designed to cure mice of mammary tumors did so two to three times more frequently if the surgery was done during the time of the cycle when both progesterone and estrogen were present in high concentrations. We also found that mammary tumor growth waxes and wanes during the mouse fertility cycle, with the highest tumor growth rate at the diestrus stage and the lowest growth rate at the estrus stage (Kobayashi et al., 2002). It is logical, therefore, to suspect that the cyclic changes in sex hormonal milieu in estrous- or menstrual-cycle stages are responsible for the obvious fertility-cycle differences in tumor growth and metastatic potential after tumor resection.

Cell lines, established from human and rodent mammary tumors, are the most commonly used in vitro models for breast cancer research. Each of the cell lines has its own unique biologic features, which have facilitated cancer research in many ways. It is often challenging to establish a cancer cell line from a well-characterized primary tumor that retains its original biologic features. Primary tumor cells in culture for long periods tend to lose the unique molecular characteristics of the parent cancer. For example, sex hormone receptors may be lost or altered. These molecular alternations may subsequently change tumor biologic behavior, i.e., enhance or diminish tumor growth, invasion, or metastatic potential (Hambly et al., 1997). To study the influence of fertility cycle and sex hormone modulation of tumor surgical curability, it is best done in a syngenic host tumor model where the immune system remains intact. We recently succeeded in establishing a new tumor cell line from a well-characterized mouse primary mammary tumor (MTP) that can be studied in vitro and in syngenic intact host in vivo. We have demonstrated that this new breast cancer cell line retains many of the in vitro and in vivo biologic features of the original MTP tumors including fertility-cycle stage–dependent metastatic potential. The availability of in vitro and in vivo tumor systems concurrently will accelerate exploration of the mechanisms by which the estrous- or menstrual-cycle stage at the time of cancer resection affects metastatic spread and breast cancer outcome.

[1] To whom correspondence should be addressed at E-mail: patricia.wood2@med.va.gov

MATERIALS AND METHODS

Animals and housing. Female C3HeB/FeJ mice were purchased from Jackson Laboratory at 4–5 wk of age and allowed to acclimate for 2 mo until 12 wk of age. Mice were housed (four per cage) in an environmentally controlled animal facility with 12 h light alternating with 12 h dark. All experiments were in compliance with the National Institutes of Health Guide for Care and Use of Laboratory Animals and have been approved by the Institutional Animal Care and Use Committee (the Veterans Affairs Medical Center Animal Care and Use Committee).

Cell culture. In general, standard aseptic techniques of cell culture were used. Cells were grown in tissue culture incubators with a 5% CO_2 atmosphere at 37° C and passaged at confluence. Cells were cultured in Rosewell Park Memorial Institute–1640 (RPMI-1640) medium containing 5–10% fetal bovine serum (FBS, GIBCO Invitrogen Co.) and antibiotics (100 IU/ml penicillin G and 25 g/ml gentamicin). In experiments where cells were treated with sex hormones, phenol red–free medium with 5% FBS was used. The experimental controls were treated in parallel by adding the same volume of vehicle to cell culture medium.

Establishment of mouse mammary tumor cell line in vitro. A piece of fresh sterile MTP primary tumor tissue was placed in ice-cold RPMI-1640 medium immediately after surgical resection from the mouse, and a single-cell suspension was prepared by forcing the tumor tissue through a metal screen. After centrifugation at 250 × *g* for 10 min, the cell pellet was resuspended in culture medium. The single-cell suspension was seeded at a concentration of 2×10^6 viable cells in 60-mm culture dishes (Falcon, Becton Dickinson Inc., Franklin Lakes, NJ). The culture medium was first exchanged the next day, when cell attachment and spreading were observed, and then refreshed twice a week. The cultured cells were trypsinized and passed into new dishes when the cells reached confluence. The subcultures were continually maintained in the above culture medium and eventually cryopreserved at the 50th passage in liquid nitrogen according to the standard procedure for long-term storage.

Mammary tumor cell line proliferation kinetics. The doubling time of the mammary tumor cell line (MTCL) cell population at the 50th passage was determined by daily cell numeration. On Day 0, 1×10^5 viable MTCL cells were seeded in three 60-mm dishes, which had grid lines on the bottom. Cells in the selected areas of each dish were counted under a converted microscope daily, and the average cell number of three areas from each of the three dishes was calculated. The tumor cell proliferation curve was plotted, and the cell doubling time was calculated based on the curve-fitting equation (CA-Cricket Graph III).

Response to sex hormones by ^{3}H-thymidine uptake. To test the responsiveness of the tumor cells to sex hormones, MTCL cells were incubated with different concentrations of progesterone (Sigma Chemical Co., St. Louis, MO) and estradiol (Sigma). The effect of these hormones on tumor cell deoxyribonucleic acid (DNA) synthesis was determined by ^{3}H-thymidine uptake assay performed in 24-well plates (Falcon, Becton Dickinson, Lincoln Park, NJ). The cells were seeded at a concentration of 2×10^4 cells/well and incubated for 24 h in phenol red–free cell culture medium. The medium was then replaced by 1 ml fresh medium containing different concentrations of progesterone (30, 60, and 90 ng/ml) or estradiol (5, 10, and 15 pg/ml) or a mixture of progesterone (60 ng/ml) and estradiol (10 pg/ml) and incubated for 2, 4, 6, 12, 24, and 48 h. Each of these hormonal exposures was performed in sextuplicate. The range of concentrations of progesterone and estrogen was chosen as reference to the physiological concentrations of sex hormones in mice (Michael, 1976; Bergman et al., 1992). The concentrations of progesterone and estrogen at the boundary phase of the proestrus and estrus stage in mice have been reported to be 60 ng/ml and 10.8 pg/ml, respectively. One hour before cell harvesting, 0.5 μCi of methyl-^{3}H-thymidine (Amersham Pharmacia Biotech, Inc., Piscataway, NJ) was added to the wells and incubated for an additional hour. The medium was removed, and cells were washed three times with ice-cold phosphate-buffered saline (PBS) and lysed with cell lysis buffer. The radioactivity in the lysate was counted with a liquid scintillation counter (LSC-5000, Aloka, Tokyo, Japan).

Mice oopharectomy. Female mice were anesthetized with an intraperitoneal injection of ketamine (75 mg/kg), acepromazine (1 mg/kg), and xylazine (10 mg/kg). A small incision was made on one lateral side of the body, and the glistening white fat pad, which included the ovary, was pulled out. A hemostat was attached at approximately 5 mm below the uterus end, and the distal tissues were cut to remove the ovary. The surgical end was tied just beneath the hemostat, and the skin wound was then closed with a metal clip. The same procedures were performed on the other side of the body. Mice were allowed to recover from the surgery for 2–3 wk. Daily vaginal smears were performed using sterile saline washings and stained with Diff Quik (J. T. Baker, Phillipsburg, NJ). An experienced pathologist read the vaginal smears using standard criteria (Allen, 1922) to determine whether the mouse's estrous cycle was ablated.

Tumor cell inoculation. Single-cell suspension was prepared from MTP primary tumors and MTCL cell subcultures. The cell viability was determined with trypan blue (Sigma). The viable tumor cells (2×10^6) in 50 μl basic RPMI medium without serum were inoculated subcutaneously on the flank of the mice for tumor growth study or on the right hind leg of mice for surgical metastatic study using a 0.5-ml syringe with a 28G1/2 needle.

Tumor size measurement and tumor growth study. Tumor-bearing mice were observed daily after the tumor cell inoculation, and the tumor size was measured at the same time of a day by the same individual using calipers (length by width by height) until euthanasia at later stages of tumor growth. The tumor size doubling times were calculated at the exponential growth periods of both MTP and MTCL tumors (the linear ranges of the tumor growth curves) based on the curve-fitting equations (CA-Cricket Graph III).

Surgical tumor resection and metastasis study. From the second day after tumor inoculation, daily vaginal smears were performed and the mouse's estrous-cycle stage was determined. Tumors, once they became measurable, were measured daily by the same individual and were resected by hind leg amputation in one of the four estrous-cycle stages at an average tumor size of 600 mm^3 (11–12 d after tumor inoculation). Mice were then followed daily for 3–4 wk. Mice were excluded from the analysis of curability if they were found with local recurrent tumor at the surgical wounding site. The remaining animals were continually followed, sacrificed when 5% of the mice died, and autopsied. To document the presence or absence of metastatic foci, both lungs were fixed in the Bouin's fixative (PolySciences Inc.) overnight. The white tumor metastatic nodules were examined and counted under a dissecting microscope (Fisher Scientific, Pittsburgh, PA). Other sites (organs) of metastases were not grossly detected.

Preparation of tumor tissue array. Tumor tissues resected from mice in the tumor growth study were fixed in 10% buffered formalin for 24 h and embedded in paraffin. One hematoxylin and eosin (H&E)–stained section was prepared from each tumor specimen and examined by a pathologist to select vital and representative areas. This section was then aligned with the donor tumor tissue block for tissue array sampling. A tissue array instrument (Beecher Instruments, Silver Spring, MD) was used to sample and transfer the tissue cores into a predrilled hole on a recipient paraffin block. For each tumor block, triplicate tissue cores of 0.6-mm diameter were taken and arrayed side by side in the recipient block. Multiple 5-μm sections were then cut from the tissue array block, and the sections were mounted on the positive-charged glass slides (SurgiPath).

Immunocytochemical–immunohistochemical staining procedures. For immunocytochemical analyses, MTCL cells were seeded in chamber slides (LAB-TEK II chamber slides, Nalge Nunc International) at a concentration of 1×10^5 cells/ml and cultured until 80% confluence. Cells were then washed with 1× PBS for 5 min and fixed for 15 min at −20° C with cold methanol.

For immunohistochemical analyses, the tissue array sections, after deparaffinization and hydration, were heated in a microwave at 700 W in sodium citrate buffer (0.1 mol/L, pH 6.0) for 7 min twice. The slides for both immunostainings were then washed in PBS (pH 7.2) for 5 min twice. The tissue endogenous peroxidase activity was blocked by 3% H_2O_2 in PBS for 15 min. Slides were incubated with normal goat serum for 1 h at room temperature. The properly diluted primary antibodies were amounted on the sections and incubated at 4° C overnight. The secondary antibodies and AB complex (ABC staining kit, Santa Cruz Biotechnology, Santa Cruz, CA) were applied and incubated for 30 min at room temperature, respectively. Between the incubations, slides were rinsed three times (5 min each) in PBS. The color was developed by 3,3′-diaminobenzidine tetrahydrochloride, and the sections were finally counterstained with Harris' hematoxylin. The negative control staining was performed without the primary antibody incubation. The rabbit polyclonal antibodies against estrogen receptor (ER α, 1:400; ER β, 1:200), progesterone receptor (PR, reactive with both A and B subtypes, 1:400), Her2/neu (1:400), EGFR1 (1:100), BRCA1 (1:400), P53 (1:200), cyclin E (1:1000), bcl-xl (1:200), and cytokeratin (pan-cytokeratin, 1:1000) were purchased from Santa Cruz. All these antibodies are reactive to human, mouse, and rat antigens, except anti-BRCA1 and -P53, which are only mouse and rat reactive. The sections were viewed using a Zeiss microscope (Jena, Ger-

many), and images were captured using a SPOT digital camera (Diagnostic Instruments, Inc.).

Quantitative analyses of immunostaining signal in tumor cells. The tumor tissue array sections that were stained with the above antibodies were used for these quantitative analyses. The digital images from each of the tumor tissue cores were analyzed using SigmaScan Pro4 (SPSS Inc., Chicago, IL). Two areas, which were representative and consisted of only viable tumor cells, were selected from each tissue core. The objectives of measurement in each of these areas were defined and selected by an optimal preset intensity. The area and average intensity of the objectives were then measured, and total intensity was calculated as $Obj_{intensity}$ = average intensity × area. The mean of average intensity of all objectives from one tumor tissue core ($M_{intensity}$) was further calculated. The negative control slides were also measured to estimate the background stain intensity ($B_{intensity}$). We then modified the $M_{intensity}$ by subtracting the average background staining, and the final formula for calculating the $M_{intensity}$ was $M'_{intensity}$ = (log 255 − log $M_{intensity}$) − (log 255 − log $B_{intensity}$) (Wells et al., 1992; You et al., 1996). The immunostaining signal intensities ($M'_{intensity}$) of the triplicate tissue cores from the same MTP or MTCL tumors were then averaged.

Tumor blood vessel count. Tumor tissue array sections were stained with CD31 antibody (PECAM-1, 1:1000). The CD31-positive–stained tumor blood vessels were quantitatively evaluated. Images of the triplicate tissue cores from the same tumor were captured and saved in files. Numbers of the tumor blood vessels in each of the triplicate tissue cores were then counted. Average number of tumor blood vessels per area in each tumor was then calculated.

Statistical analysis. For each numerical value, such as the number of cultured tumor cells, number of tumor blood vessels, and tumor sizes, mean and standard deviation were calculated (standard errors were used in graphs). Comparison between two groups was done by *t*-test, and comparison between the means was done by one-way analysis of variance with significance at $P < 0.05$.

Results

Establishment of MTCL in vitro. MTP tumor cells (2×10^6) were inoculated subcutaneously on the flank of a 3-mo-old female C3HeB/FeJ mouse. Two weeks later, the tumor was resected, and a single-cell suspension was prepared from the most vital part of the tumor. These tumor cells were then seeded in a 60-mm culture dish with RPMI culture medium. The culture medium was replaced on the second day of culture, when some of the cells had adhered to the bottom of the culture dish. The shapes of the cells at this point were highly heterogeneous. After the first replacement, the medium in the culture dish was refreshed twice a week. The cultured cells, when they reached confluence, were trypsinized and passaged into new dishes. At the 50th cell passage, the cell population was quite uniform. An epithelial-like tumor cell population (MTCL) became predominant. These epithelial tumor cells were polygonal in shape, varied in size, and were positive for cytokeratin immunostaining, as are typical of malignant epithelial cells (Fig. 1). Although other cells, i.e., fibroblast cells (long, spindle in shape) and small mononucleated cells (spheroid in shape), were observed at earlier stages of the culture, the number of these cells decreased during successive cell passages, and very few fibroblast-like cells were found between the malignant epithelial cells at the 50th passage. To estimate the proliferative rate of MTCL cells, we seeded equal numbers of MTCL tumor cells into triplicate dishes. We counted the cell numbers in selected areas daily. MTCL cells had a typical lag phase at the beginning of the culture and then grew exponentially after a day or two (Fig. 2). The cell doubling time at the linear range of the tumor cell proliferation curve was estimated to be 41 h.

Expression of ER and PR proteins and response to sex hormones in vitro. Expression of sex hormone receptors, ER and PR, is a major biochemical characteristic of the original MTP mammary tumor cells. To determine if MTCL tumor cells retained expression of ER and PR, we cultured the cells in chamber slides and then stained the cultured tumor cells with anti–ER α, anti–ER β, and anti-PR antibodies immunocytochemically. Figure 3 shows that most of the MTCL cells express ER α, ER β, and PR at the 50th

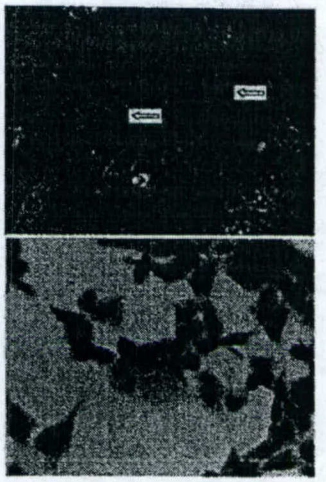

FIG. 1. Mammary tumor cell line (MTCL) cell morphology in vitro. At the 50th passage of cell culture, MTCL mammary tumor cells became a predominate cell population with triangular or polygonal cell shapes (*a, arrows,* ×40 phase objective lens), and some of the cells are strongly stained with a pan-cytokeratin antibody, typical features of epithelial cells (*b,* ×40 light objective lens).

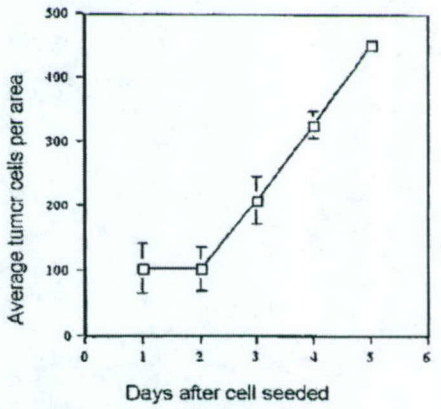

FIG. 2. In vitro growth kinetics of mammary tumor cell lines (MTCL) cells. MTCL cells were seeded in triplicate dishes, and cell number was quantitated in selected areas daily. The cultured MTCL cells showed a slow initial increase in cell number and then proliferated exponentially. The cell population doubling time at the linear range of the growth curve is 41 h, calculated based on the curve-fitting equation, $Y_{d1-d5} = 116.4X_{d1-d5} - 134.7$. Values are means ± standard errors.

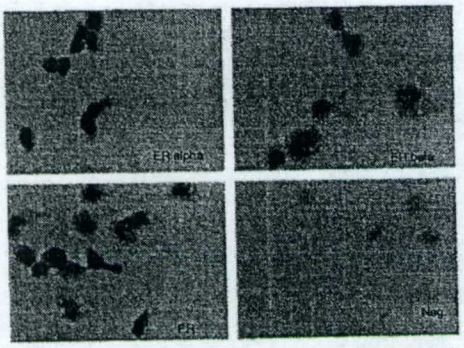

FIG. 3. In vitro sex hormone receptor expression in mammary tumor cell line (MTCL) cells. MTCL tumor cells were cultured in chambered glass slides and stained immunocytochemically with estrogen receptor (ER) α, ER β, and progesterone receptor antibodies. Most of the MTCL cells are positively stained with these antibodies. The positive signals are mainly found in the nucleus (darker brown) and some are found in the cytoplasm (lighter brown). In negative control slides (3_{neg}), there is no positive staining. The cell nuclei are in blue (×40 light objective lens).

passage of the culture. These receptors are mainly found within the cell nucleus; yet, some of them are seen in the cytoplasm.

To evaluate the responsiveness of MTCL cells to sex hormones, we exposed the cells in vitro to different concentrations of progesterone (30, 60, and 90 ng/ml) and estradiol (5, 10, and 15 pg/ml) for 2, 4, 6, 12, 24, and 48 h and then determined the ^{3}H-thymidine uptake to assess whether hormone exposure affected the tumor cellular DNA synthesis. Exposing MTCL cells to progesterone alone diminished cell capacity to take up ^{3}H-thymidine (Fig. 4a). The ^{3}H-thymidine uptake in progesterone-exposed MTCL cells was significantly lower when compared with that of the vehicle-exposed cells ($P < 0.01$). Conversely, exposing MTCL cells to a higher dose of estradiol (15 pg/ml) for 48 h increased the rate of ^{3}H-thymidine uptake ($P = 0.045$), although there were no changes in ^{3}H-thymidine uptake with lower doses of estrogen exposures (Fig. 4b) (5 and 10 pg/ml, $P > 0.05$). We also exposed MTCL tumor cells to a combination of progesterone (60 ng/ml) and estradiol (10 pg/ml) for different times (2, 4, 6, 12, 24, and 48 h). Similar to the case of exposing MTCL cells to progesterone alone, the combination of progesterone (60 ng/ml) and estradiol (10 pg/ml) significantly decreased the rates of MTCL cell ^{3}H-thymidine uptake, indicating that the effect of progesterone on MTCL cellular ^{3}H-thymidine incorporation was dominant (Fig. 4c).

In vivo tumor growth. We inoculated 2×10^6 MTCL syngenic tumor cells subcutaneously on the flank of five ovx mice to test their tumorigenicity. As a parallel control, the same number of viable MTP original primary tumor cells was inoculated in another group of five ovx mice. We monitored the tumor growth daily for more than 3 wk and sacrificed the mice at later stages of tumor growth. About 10 d after MTCL tumor cell inoculation, a palpable tumor was first found in three of the five mice. Two days later, a measurable tumor was formed in the other two mice. The average time for initial MTCL tumor appearance was 11 d (Fig. 6), 4 d later than the average initial appearance of the original MTP tumors. After the initial appearance, however, MTCL tumor growth was faster than MTP tumor growth. The MTCL tumor size in vivo doubling time at the linear growth phase was about 31 h, 10.8 h shorter than that of MTP tumors (41.8 h). At late stages of tumor growth, MTP tumor–bearing mice began to show apparent body fat loss, slowed motion, and ruffled hair appearance, at which point they were euthanized. However, at similar tumor sizes, mice with MTCL tumors demonstrated normal eating, grooming, and activity without apparent loss of body fat. All five of the MTCL tumor–bearing mice were physically well, even though they were bearing bigger tumors.

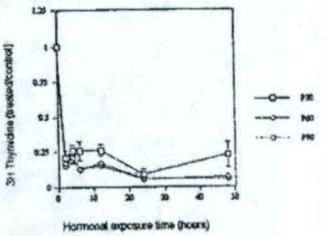

4a

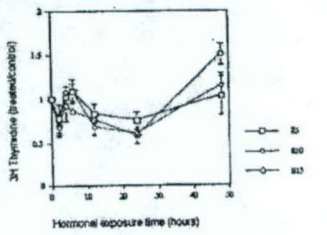

4b

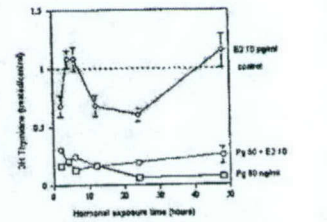

4c

FIG. 4. In vitro ^{3}H-thymidine incorporation. Dose and time course of ^{3}H-thymidine uptake of mammary tumor cell line (MTCL) cells in response to progesterone (a), estrogen (b), and progesterone plus estrogen (c). To compare the capacity of ^{3}H-thymidine uptake among different exposure times, we normalized each of the ^{3}H-thymidine radioactivities from sex hormone–treated samples as the ratio to background radioactivity from corresponding control cells. Progesterone (P) was used at 30, 60, and 90 ng/ml and estrogen (E) at 5, 10, and 15 pg/ml. Values are means ± standard errors.

Fertility-cycle–dependent surgical curability of MTP and MTCL tumors. The fertility-cycle stage at primary tumor resection, as we

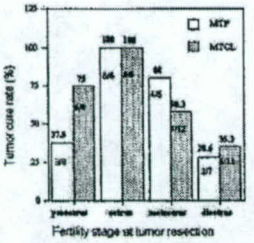

FIG. 5. Surgical cure rates with primary tumor resection performed at different estrous-cycle stages (proestrus, estrus, metestrus, and diestrus) for MTP and mammary tumor cell line tumors. Numbers within the *bars* are the number of cured mice/total mice.

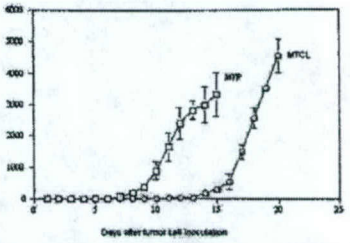

FIG. 6. Tumor growth kinetics in vivo. MTP or mammary tumor cell line (MTCL) cells were inoculated into oophorectomized mice ($n = 5$ mice/group) and tumor sizes were measured daily. The average initial time to appearance of MTCL tumor was 11 d, 4 d longer than that of MTP tumors (7 d). After tumor initial appearance, however, MTCL tumors grew faster than MTP tumors did. The exponential phase of tumor growth (the linear ranges of the growth curves—Day 7 to Day 13 for MTP tumor, Day 15 to Day 20 for MTCL tumor) was chosen for curve-fitting analyses, and tumor doubling times were calculated based on the following equations: $Y_{MTP} = 574X_{MTP} - 4642.6$, $Y_{MTCL} = 773X_{MTCL} - 11{,}258.3$. The tumor doubling time of MTCL tumor is about 31 h, 10.8 h shorter than that of MTP tumors (41.8 h). Values are means ± standard errors.

have reported previously (Ratajczak et al., 1988; Bove et al., 2002), affects the MTP tumor distant metastatic recurrence rate. To compare the metastatic potential of MTCL tumors with that of original MTP tumors, we inoculated MTP or MTCL tumor cells into the right hind leg of two groups of normal cycling mice (34 mice in one and 42 mice in another). Both tumor and leg were resected when the tumor grew to an average size of 600 mm³ (11–12 d after tumor inoculation), and the tumor-bearing mice were observed for an additional 3–4 wk, at which time they were euthanized to screen for lung metastases. In both tumor models, a fixed rate of local tumor recurrence was seen. We found that 23.5% of mice with MTP tumor and 31% of mice with MTCL tumors developed early local recurrence after resection. The local tumor recurrent rates demonstrated no association with the time of tumor resection within mouse fertility stages (MTP tumor, $P = 0.554$; MTCL tumor, $P = 0.215$). The mice without local recurrent tumors were continually followed, sacrificed, and autopsied later to score for the lung metastases. We demonstrated that 42.3% of mice with resected MTP tumors and 42.8% of mice with resected MTCL tumors developed lethal lung metastases. Excluding local recurrences, surgical cure rates were 28.6 and 35.3% when the MTP and MTCL tumor resection surgeries, respectively, were performed within the diestrus stage, whereas 100% cure rates were found in both groups of mice when the MTP and MTCL tumor resection surgeries were performed within the estrus stage (Fig. 5). The surgical cure rates of MTCL and MTP tumors were significantly associated with the surgical time within mouse estrous-cycle stages ($P = 0.044$, $P = 0.027$) with nearly identical patterns in both tumor types. This biologic behavior is identical to that reported previously (Ratajczak et al., 1988; Bove et al., 2002).

Comparative histology of the MTP and MTCL tumors. Tumor tissues from the growth study of ovx mice were immediately evaluated grossly after they were dissected from the mice. The MTCL tumors appeared as encapsulated subcutaneous tumors with little invasion of underlying tissues. On gross inspection, instead of extensive necrosis, a typical feature of MTP tumors, MTCL tumors demonstrate only small patches of necrosis. These findings were supported by microscopic comparison of the H&E-stained tumor sections (Fig. 7*a* and *b*). The vital parts of both tumors, however, have similar light microscopic characteristics. Both tumors express cytokeratin protein (Fig. 7*c* and *d*) and consist of typical undifferentiated malignant epithelial cells.

Comparative in vivo breast cancer protein expression. Each of the

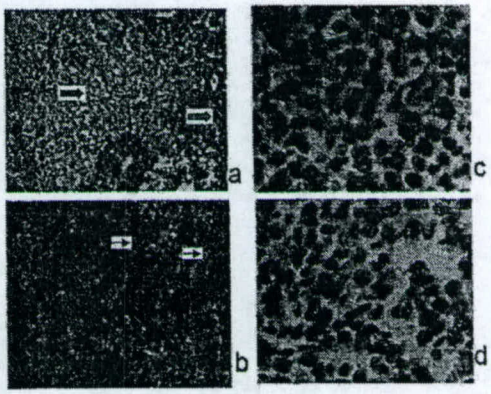

FIG. 7. Histological features of MTP and mammary tumor cell line (MTCL) tumors. Sections were prepared from MTP and MTCL tumor blocks and stained with hematoxylin and eosin. MTP tumors show interdispersed patches of necrosis (*a*, *dark blue arrow*) with smaller areas of viable tumor tissues (*a*, *light blue arrow*), whereas MTCL tumors show much less necrosis and more numerous blood vessels (*b*, *small arrows*). The cancer cells in both tumors appear as undifferentiated malignant epithelial cells (*a* and *b*, ×10 light objective lens). Both MTP and MTCL tumors are strongly pan-cytokeratin positive (*c* and *d*, ×40 light objective lens).

five MTP and MTCL tumor tissues were fixed in formalin and embedded in paraffin blocks. Sample H&E slides were inspected, and viable areas of predominant tumor cells were selected for more detailed studies. A tissue array block was created by biopsy of each tumor block at these microscopically optimal areas. Thirty tissue cores (three from each tumor sample) were arrayed side by side. Sections of this tissue array were cut and prepared for immunohistochemical assessment of key tumor proteins. The expressions of all the selected target proteins in all tumor tissues were first assessed

TABLE 1

COMPARATIVE IN VIVO PROTEIN EXPRESSION IN MTP AND MTCL TUMORS AS ASSESSED BY IMMUNOHISTOCHEMICAL STAINING AND DIGITAL IMAGING QUANTITATION[a,b]

	Sex hormone receptors			Epithelial receptors		Tumor suppressors		Proliferation and apoptosis	
	ER α	ER β	PR	neu[c]	EGFR1	P53	BRCA1	Cyclin E	bcl-xl
MTCL									
OD	0.26	0.22	0.21	0.21	0.20	0.19	0.20	0.12	0.21
SE	0.02	0.02	0.01	0.01	0.02	0.02	0.02	0.01	0.01
MTP									
OD	0.30	0.26	0.20	0.23	0.24	0.22	0.24	0.18*	0.23
SE	0.02	0.02	0.01	0.02	0.03	0.01	0.03	0.01	0.02

[a] MTP, primary mammary tumor; MTCL, mammary tumor cell line; ER, estrogen receptor; PR, progesterone receptor; OD, mean optical density (see *Material and Methods*); SE, standard error.
[b] Values are based on a log scale.
[c] Her2/neu.
* P value less than 0.01 for MTCL compared with MTP.

under the microscope and then quantitatively measured by digital image analysis. Sex hormone receptors (ER α, ER β, and PR) were expressed at equivalent levels in both MTP and MTCL tumors. Proteins related to epithelial growth hormonal receptors (Her2/neu, EGFR1), tumor suppression (BRCA1, P53), and cell apoptosis (bcl-xl) were also expressed at similar levels in both tumors (Table 1). The signal intensity of the cyclin E_0 immunostain, however, was significantly higher in MTP tumor cells than that in MTCL tumor cells. This immunostaining difference was also obvious under microscopic observation.

Tumor blood vessels in MTP and MTCL tumors. Because of large differences seen in tumor necrosis in these two tumors types, tumor angiogenesis in these tumors was quantitatively evaluated by staining tissue array sections with a polyclonal anti-CD31 antibody, previously shown to allow the quantitative assessment of tumor blood vessels (Bevilacqua et al., 1995; Laforga and Aranda, 2000). This staining demonstrated vascular endothelial cells and outlined the shapes of tumor blood vessels, which appeared in round or ovoid shapes (Fig. 8). In some of the tumors, the blood vessels were extremely dilated, but in other cases, they were very narrow so that blood vessels appeared as endothelial cell cords. Tumor cells around the blood vessels appeared more robustly viable than those farther from the vessels; when necrosis occurred, it was always far from these CD31-positive areas. The total number of tumor blood vessels in each of the tumor cores was counted and averaged with the triplicate core specimens from the same tumor paraffin block because each core was of identical size and shape. MTCL tumors were significantly more vascularized than MTP tumors. The average number of blood vessels in MTCL tumors was 5.4 ± 1.6 per core, whereas that in MTP tumors was 3.4 ± 1.2 per core (P = 0.0343). Tumor cells (both types of tumors) as well as other types of the normal interstitial cells adjacent to blood vessels expressed little or no CD31 protein.

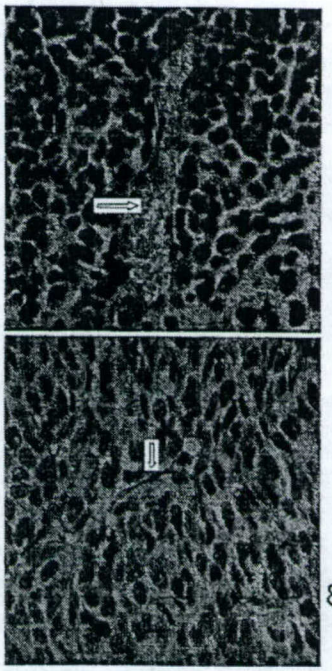

FIG. 8. Tumor angiogenesis in MTP and mammary tumor cell line (MTCL) tumors. Sections were prepared from MTP and MTCL tissue array blocks and stained with anti-CD31 antibody. The tumor blood vessels are shown clearly between tumor cells with various shapes, i.e., ovoid lumens (*a*) or very narrow and thin capillaries (*b*) (×40 light objective lens), and are more numerous in MTCL tumors than in MTP tumors.

DISCUSSION

Bernard Fisher's compelling work demonstrating the importance of host factors in determining whether lethal metastases develop was done with the parent MTP murine mammary tumor in the late 1950s (B. Fisher and E. Fisher, 1959; Fisher et al., 1968). Fisher

observed and documented that tumor dormancy and spread was interrupted by surgery, resulting in postsurgical metastatic cancer growth. Subsequent work of Pollock and Lotzova demonstrated transient yet profound cellular immunoparalysis in both mice and patients after surgery (Pollock and Lotzova, 1987; Pollock et al., 1987). We have investigated the interrelationship among host, surgery, tumor, and the fertility cycle. Our experiments with Fisher's breast cancer model demonstrate that the timing of potentially curative cancer resection within the fertility cycle determines the metastatic potential of that cancer and the ultimate curability of that mouse (Ratajczak et al., 1988; Bove et al., 2002).

The levels of sex hormones dynamically change during the female fertility cycle and affect the cellular proliferation in both the nulliparous murine mammary gland (Fata et al., 2001) and breast cancer (Badwe et al., 1995; Saad et al., 1998). In the normal murine mammary gland, Fata et al. (2001) demonstrated specific morphological and cellular changes in the breast during each estrous cycle and defined their relationship to rhythmic physiological changes in steroid hormone concentration. They found that the mammary epithelial cell proliferation and apoptosis correlated better with progesterone than 17β-estradiol serum concentrations. They proposed that the cyclical turnover of epithelial cells within adult mammary tissue is a sum of spatial and functional coordination of sex hormonal and matrix regulatory factors, e.g., the matrix metalloproteinases and their specific tissue inhibitors (TIMPs). In human breast cancer, several studies measuring tumor growth and metastasis-relevant gene expression (Badwe et al., 1995; Saad et al., 1998; Balsari et al., 1999) have correlated lower metastatic potential and favorable outcome with high progesterone levels, which occur in the early luteal phase of each menstrual cycle. Therefore, our demonstration of the responsiveness of MTCL tumor cells to progesterone is a reasonable step toward determining whether this newly established cell line remains useful for the chronobiologic study of breast cancer. The effect of progesterone on cell proliferation and apoptosis of human and mouse breast cancer in vitro has been controversial. Moore et al. (2000) and Ory et al. (2001) have reported that progesterone has an antiapoptotic or proproliferative effect in vitro on PR-rich human breast cancer cells (TD47). Exposing TD47 tumor cells to progestins induced upregulation of the antiapoptotic protein bcl-xl expression. Formby and Wiley (1998, 1999) and Gompel et al. (2000) have, however, reported proapoptotic effects. Formby and Wiley (1998, 1999) demonstrated a maximal 90% inhibition of cell proliferation with TD47 breast cancer cells (PR+) after exposure to 10 μM progesterone for 72 h, whereas control MDA-231 cancer cells (PR−) were unresponsive to the progesterone exposure. We have demonstrated that progesterone obviously inhibits MTCL tumor cell DNA synthesis. This result is consistent with the results of Formby and Wiley (1998, 1999) and Gompel et al. (2000) and differs from those of Moore et al. (2000) and Ory et al. (2001).

One of the most interesting features of the primary MTP tumor model is the dependence of tumor metastatic spread after resection on the estrous-cycle stage of this resection. To test if the newly established MTCL tumor cells retain this unique biologic feature, we inoculated MTP and MTCL tumor cells in separate groups of mice and resected their tumor for cure. We measured local tumor recurrence and lung metastatic spread and found that the estrous-cycle dependence of tumor metastatic potential after resection was identical for both tumors. Tumor resection during estrus stage resulted in the highest curability in both types of tumors, whereas resection during the diestrus stage resulted in the lowest cancer curability. The idea of resecting breast cancer at the defined menstrual- or estrous-cycle stage to improve outcome originally arose from Ratajczak's study using MTP tumor model (Ratajczak et al., 1988), which then stimulated many clinical studies. Since Hrushesky published the first clinical study in 1989 (Hrushesky et al., 1989), many well-designed clinical studies involving thousands of breast cancer patients have shown that disease-free or overall survival is reduced after surgery in the follicular phase compared with the luteal phase (Hagen and Hrushesky, 1998), whereas some other studies found no correlation between timing of surgery in relation to the menstrual cycle and prognosis of premenopausal patients with breast cancer (Kroman et al., 1994; Nomura et al., 1999). Recent works by Bove et al. (2002) and Vantygham et al. (2003) further confirmed this concept. In two large independent studies, Bove et al. (2002), using the same strain of mice and same tumor model as Ratajczak did, demonstrated 100 and 93% surgical cure rates when the tumor was resected during estrus stage versus 40 and 47% surgical cure rates during the diestrus stage. In another study, Vantygham et al. (2003) delivered B16F10 melanoma cells into C57BL/B6 mouse circulation through tail vein injection at two different estrous-cycle stages, the proestrus and metestrus stages. As expected, there was a large metastatic burden in the lung at 24 d after tumor cell injection, although the number and size of lung metastases did not differ between two injection stages. Unexpectedly, however, they found dramatic differences in extrapulmonary metastases between the different stages of injection. A total of 31.6% of mice injected in metestrus stage had ovarian metastases, whereas none of the mice injected during the proestrus stage had ovarian metastasis. They proposed that the fertility-cycle timing of surgery may be more broadly applicable than to just breast cancer.

Subcutaneous tumor growth in the ovx mice was monitored daily and the growth kinetics of MTCL tumor in vivo was found to be somewhat different from that of MTP tumor. MTCL tumor had a longer average time to initial appearance compared with those of the original MTP tumors. There are several possible explanations for the slow initial growth of MTCL tumors. First, MTP tumor is a primary tumor line, which is usually considered a heterozygous tumor containing multiple subpopulations with different growth potential. MTCL may be derived from one of the subpopulations with slower growth potential. Second, MTP tumor cell suspension contains a number of interstitial cells, such as fibroblasts, endothelial cells, macrophages, and lymphocytes. These cells are not only the passive witnesses of the tumor proliferation cascade but also may modulate tumor establishment and growth in vivo. Through secretion of their soluble (cytokines) and insoluble molecules (extracellular matrix), interstitial cells mutually modulate tumor growth in vivo (Duffy et al., 2000; Hirtenlehne et al., 2002). Third, the dose of injected tumor cells is another factor that may affect the initial tumor appearance, as described by Hrushesky et al. (1999). To avoid injecting large number of necrotic MTP tumor cells and to make a valid comparison with MTCL tumor cells, we made tumor cell suspensions from the most vital part of MTP tumor and injected the same number of viable MTP and MTCL tumor cells into mice. We, therefore, believe that the initial appearances of the tumors truly reflect their different growth potentials.

Long-term in vitro culture exerts selective pressure on the cultured tumor cells (Hambly et al., 1997). This pressure may change or alter the molecular pathways within the tumor cells. We com-

pared the molecular fingerprints of the newly established MTCL-derived tumors with those of the original MTP tumors. Eight of nine proteins, such as sex hormone receptors (ER α, ER β, and PR) as well as proteins of several important epithelial growth factor receptors (Her2/neu, EGFR1), tumor suppressor genes (P53, BRCA1), and the gene that is relevant to cell apoptosis (bcl-xl) are all expressed equally in both parent and cell line–derived tumors. This largely similar protein expression profile may account for, at least in part, the comparable metastatic potential of MTP and MTCL tumors. Cyclin E is the only protein that is expressed differently in these two types of tumors. The average intensity of cyclin E immunostaining in MTP tumors is much higher than that in MTCL tumors, indicating the higher expression level of this cell proliferation–relevant protein in MTP tumors. Considering the obvious necrosis in the late stage of MTP tumors and overexpressed cyclin E protein, we assume that MTP tumor cells have a faster tumor turnover rate than MTCL tumor cells. At early tumor growth stages, MTP tumor expresses more cell proliferation–relevant proteins, i.e., cyclin E, resulting in faster tumor growth and earlier initial tumor appearance. At later stages of MTP tumor growth, however, tumor necrosis becomes apparent, which slows the speed of tumor size increase. On the contrary, MTCL tumor does not show apparent necrosis because the tumor has a high density of tumor blood vessels.

In summary, we have established a new MTCL from a well-defined mouse primary mammary tumor, which can be studied both in vitro and in vivo. This cell line expresses cytokeratin, ER, and PR proteins and responds markedly to progesterone exposures in vitro. Like the parent tumors, MTCL tumors demonstrated very similar molecular expression profiles, histological features, metastatic potential, and fertility-cycle dependence of postresection recurrence in vivo. Availability of this tumor cell line, with its unique in vivo biologic characteristics, will enable chronobiologists to construct studies to determine the relationship of sex hormone exposure and tumor cell proliferation and apoptosis and further investigate the interaction between estrous- or menstrual-cycle stages and tumor growth and metastatic spread.

Acknowledgments

We thank Dr. B. Fisher for providing us the original MTP murine mammary tumor line, Dr. K. Creek for his valuable suggestions and consultations, and Dr. B. Price for the core facility supports. We also thank all summer students who attended this work, J. Quiton, S. Bickley, X. You, and C. Hrushesky. This work is supported by South Carolina Cancer Research Fund 18300 KA05 (S. Y.), Veterans Affairs (VA) career developing award VISN 7 CDA (S. Y.), research fund from Mochida Memorial Foundation for Medical and Pharmaceutical Research (M. K.), VA merit award Type I fund (P. W.), VA merit award Type I fund (W. H.), and Department of Defense breast cancer research fund DAMD17-98-1-8016 (W. H.).

References

Allen, E. The oestrous cycle in the mouse. Am. J. Anat. 30:297–348; 1922.

Badwe, R. A.; Bettelheim, R.; Millis, R. R.; Gregory, W.; Richards, M. A.; Fentiman, I. S. Cyclical tumour variations in premenopausal women with early breast cancer. Eur. J. Cancer 31A:2181–2184; 1995.

Balsari, A.; Casalini, P.; Tagliabue, E., et al. Fluctuation of HER2 expression in breast carcinomas during the menstrual cycle. Am. J. Pathol. 155:1543–1547; 1999.

Beatson, G. On the treatment of inoperable cases of carcinoma of the mamma: suggestions for a new method of treatment with illustrative cases. Lancet 2:104–107; 1896.

Bergman, M.; Schachter, B. S.; Karelus, K.; Combatsiaris, E.; Garcia, T.; Nelson, J. Up-regulation of the uterine estrogen receptor and its messenger ribonucleic acid during the mouse estrous cycle: the role of estradiol. Endocrinology 130:1923–1930; 1992.

Bevilacqua, P.; Barbareschi, M.; Verderio, P., et al. Prognostic value of intratumoral microvessel density, a measure of tumor angiogenesis, in node-negative breast carcinoma—results of a multiparametric study. Breast Cancer Res. Treat. 36:205–217; 1995.

Bove, K.; Lincoln, D. W.; Wood, P. A.; Hrushesky, W. J. Fertility cycle influence on surgical breast cancer cure. Breast Cancer Res. Treat. 75:65–72; 2002.

Duffy, M.; Maguire, T. M.; Hill, A.; McDermott, E.; O'Higgins, N. Metalloproteinases: role in breast carcinogenesis, invasion and metastasis. Breast Cancer Res. 2:252–257; 2000.

Fata, J.; Chaudhary, V.; Khokha, R. Cellular turnover in the mammary gland is correlated with systemic levels of progesterone and not 17beta-estradiol during the estrous cycle. Biol. Reprod. 65:680–688; 2001.

Fisher, B.; Fisher, E. Experimental evidence in support of the dormant tumor cell Science. Science 130:918–919; 1959.

Fisher, B.; Ravdin, R. G.; Ausman, R. K.; Slack, N. H.; Moore, G. E.; Noer, R. J. Surgical adjuvant chemotherapy in cancer of the breast: results of a decade of cooperative investigation. Ann. Surg. 168:337–356; 1968.

Formby, B.; Wiley, T. S. Progesterone inhibits growth and induces apoptosis in breast cancer cells: inverse effects on Bcl-2 and p53. Ann. Clin. Lab. Sci. 28:360–369; 1998.

Formby, B.; Wiley, T. S. Bcl-2, survivin and variant CD44 v7-v10 are down-regulated and p53 is upregulated in breast cancer cells by progesterone: inhibition of cell growth and induction of apoptosis. Mol. Cell. Biochem. 202:53–61; 1999.

Gompel, A.; Somai, S.; Chaouat, M., et al. Hormonal regulation of apoptosis in breast cells and tissues. Steroids 65:593–598; 2000.

Hagen, A. A.; Hrushesky, W. J. Menstrual timing of breast cancer surgery. Am. J. Surg. 175:245–261; 1998.

Hambly, R.; Double, J. A.; Thompson, M. J.; Bibby, M. C. Establishment and characterisation of new cell lines from human breast tumours initially established as tumour xenografts in NMRI nude mice. Breast Cancer Res. Treat. 43:247–258; 1997.

Hirtenlehne, K.; Pec, M.; Kubista, E.; Singer, C. F. Extracellular matrix proteins influence phenotype and cytokine expression in human breast cancer cell lines. Eur. Cytokine Netw. 13:234–240; 2002.

Hrushesky, W. J.; Bluming, A. Z.; Gruber, S. A.; Sothern, R. B. Menstrual influence on surgical cure of breast cancer. Lancet 2:949–952; 1989.

Kobayashi, M.; You, S.; Wood, P.; Hrushesky, W. Prominent circadian and estrous cycle impact upon tumor biology. "Circadian Rhythms and Sleep: View to the Future" Jacsonville, FL. Eighth Meeting Society for Research on Biological Rhythms; 2002.

Kroman, N.; Hojgaard, A.; Andersen, K. W., et al. Timing of surgery in relation to menstrual cycle does not predict the prognosis in primary breast cancer. Danish Breast Cancer Cooperative Group. Eur. J. Surg. Oncol. 20:430–435; 1994.

Laforga, J.; Aranda, F. I. Angiogenic index: a new method for assessing microvascularity in breast carcinoma with possible prognostic implications. Breast J. 6:103–107; 2000.

Michael, S. D. Plasma prolactin and progesterone during the estrous cycle in the mouse. Proc. Soc. Exp. Biol. Med. 153:254–257; 1976.

Moore, M.; Conover, J. L.; Franks, K. M. Progestin effects on long-term growth, death, and Bcl-xL in breast cancer cells. Biochem. Biophys. Res. Commun. 277:650–654; 2000.

Nomura, Y.; Kataoka, A.; Tautsui, S.; Murakami, S.; Takenaka, Y. Lack of correlation between timing of surgery in relation to the menstrual cycle and prognosis of premenopausal patients with early breast cancer. Eur. J. Cancer 35:1326–1330; 1999.

Ory, K.; Lebeau, J.; Levalois, C.; Bishay, K.; Fouchet, P.; Allemand, I.; Therwath, A.; Chevillard, S. Apoptosis inhibition mediated by medroxyprogesterone acetate treatment of breast cancer cell lines. Breast Cancer Res. Treat. 68:187–198; 2001.

Pollock, R.; Lotzova, E. Surgical-stress-related suppression of natural killer cell activity: a possible role in tumor metastasis. Nat. Immun. Cell Growth Regul. 6:269–278; 1987.

Pollock, R.; Lotzova, E.; Stanford, S. D.; Romsdahl, M. M. Effect of surgical stress on murine natural killer cell cytotoxicity. J. Immunol. 138:171–178; 1987.

Ratajczak, H. V.; Sothern, R. B.; Hrushesky, W. J. M. Estrous influence on surgical cure of a mouse breast cancer. J. Exp. Med. 168:73–83; 1988.

Saad, Z.; Bramwell, V.; Wilson, S.; O'Malley, F.; Jeacock, J.; Chambers, A. Expression of genes that contribute to proliferative and metastatic ability in breast cancer resected during various menstrual phases. Lancet 351:1170–1173; 1998.

Vantyghem, S.; Postenka, C. O.; Chambers, A. F. Estrous cycle influences organ-specific metastasis of B16F10 melanoma cells. Cancer Res. 63:4763–4765; 2003.

Wells, W.; Rainer, R. O.; Memoli, V. A. Basic principles of image processing. Am. J. Clin. Pathol. 98:493–501; 1992.

You, S.; Yao, K.; Cao, Y. Latency of Epstein-Barr virus and its relationship to nasopharyngeal carcinomas. Zhonghua Zhongliu Zazhi 18:23–26; 1996.

Sex Cycle Modulates Cancer Growth

Patricia A. Wood and William J.M. Hrushesky*

Dorn Veterans Affairs Medical Center

Columbia, SC

Supported in part by VA Merit Award (WJMH and PAW), National Institutes of Health grant RO1 CA31635 and RO1 CA50749 (WJMH), NYS Breast Cancer Research Program grant, **ARMY IDEA grant #17-98-1-8016**, VA Merit Award (WJMH), Robison Family Foundation.

*Corresponding Author: WJMH - Dorn VAMC, 6439 Garners Ferry Road. Columbia, SC 29201
Phone: 803-695-6825, ext. 2792, Fax 803-695-6829, email: william.hrushesky@med.va.gov

We wish to thank Hemant Gupta, MD, for his help for endlessly measuring tumors and making estrous smears, Dr. Shaojin You, MD, PhD, for determining the estrogen and progesterone receptor status of both tumors and Jovelyn Du-Quiton for data analysis and graphic presentation.

ABSTRACT

Hypothesis: Among premenopausal women, both metastatic potential and tumor growth rate are governed by the menstrual cycle. There is strong support for the former in large retrospective studies and the following experiments were conducted to evaluate the later.

Methods: We studied a transplantable breast cancer of C3HeB/FeJ mice (3 studies), and a transplantable methylcholantherene induced sarcoma of CD2F1 mice (2 studies). We concurrently measured local cancer size and estrous cycle stage up to twice and at least once each day. There is a natural individual variability in the average length of normal estrus (3-1/2 to 7 days) cycle in mice. We assessed the effect of the cycle stage and duration on average tumor growth rate.

Results: We found identical estrous cycle stage coordination of cancer size across all studies in these tumors which are both estrogen receptor alpha and progesterone receptor positive. Little or no change in cancer size occurs during proestrus (preovulatory phase) and estrus (periovulatory phase); tumor size increases several fold during diestrus (post-ovulatory phase); and the tumor shrinks partially as the next proestrus phase is approached. Across both mouse strains and tumor types, mice whose average cycle length is briefer (faster cyclers), have s lower a verage t umor growth rate than those with longer cycles (slower cyclers) who have faster tumor growth rates.

Conclusion: The virtually identical modulation of tumor size and cancer growth rate, in each of two very different transplantable cancers (one, classically sex-hormone-dependent, and the other, never previously recognized as hormone dependent) growing in two unrelated inbred mouse strains, indicates that the fertility cycle related host factors affect cancer size and growth rate. These findings predict that the biology of both breast and non-breast cancers in premenopausal women may be meaningfully affected by the menstrual cycle.

Key words: Breast Cancer • Fertility Cycle • Chronobiology • Estrous Cycle •Metastases • Sex Hormone

INTRODUCTON

Sex affects cancer outcome. The outcome for adult cancers affecting both sexes is superior in women. The younger the median age at diagnosis, the greater the female advantage.[1,2] Most childhood cancers show no advantage for female sex until puberty. Interestingly, this female advantage is confined largely to cancers whose outcomes are influenced most by metastatic tumor dissemination and those cancers treated mainly by tumor resection. These include epithelial tumors and sarcomas. Epidemiologic data connect menstrual cycle characteristics with cancer outcome. The normal menstrual cycle duration varies from woman to woman between ~ 21 and ~ 35 days.[3] The risk of developing breast cancer varies with the average length of the menstrual cycle. The shorter the woman's cycle (the faster she cycles), the lower the breast cancer risk.[4,5]

Experimental carcinogenesis data also support this connection between cancer and the fertility cycle. Breast tumor incidence, tumor latency, and number of tumors induced by the direct carcinogen, N-methyl nitrosourea (NMU) and an indirect carcinogen, 7,12-dimethylbenzanthracene each depend upon the estrous cycle phase at the time of carcinogen administration. [6-8] The frequency of tumor cell, H-*ras* proto-oncogene mutation in these NMU-induced tumors is likewise dependent upon the estrous cycle stage of NMU exposure.[9]

Sex hormones also affect the host-surgery-cancer interaction. When a transplantable mammary carcinoma of C3HeB/FeJ mice is surgically removed after several weeks of growth, not every mouse is cured and some die subsequently from metastases, not unlike the human situation.[10] The timing within the fertility cycle of surgical resection of this same size primary C3H breast tumor influences whether subsequent metastases occur.[11] An estrogen- and progesterone receptor-positive mammary cell line, derived from this primary tumor, also demonstrates this same estrous cycle dependence of surgical curability.[12] Host factors may be responsible for much of this cyclical tumor biology. For example, splenocyte natural killer (NK) cell activity and interleukin-2 (IL-2) production, in tumor-free C3HeB/FeJ mice, vary throughout the cycle. The cycle stages associated with the lowest metastatic potential, demonstrate the highest NK activity and IL-2 production.[13] Women resected during the putative early luteal phase of their menstrual cycles have a better chance of surviving than those women whose breast cancers were resected in the follicular phase, during or nearer to menses.[14] The dozen most

complete retrospective studies indicate that optimal resection timing may enhance 10 year disease free survival by an average of 25% in absolute terms.[15,16] A total of more than 40 subsequent retrospective studies of more than 10,000 women have largely, but not unanimously, supported these clinical observations.[16] A single ongoing prospective study has so far partially confirmed this biology.[17,18]

We now present data in this same C3H murine breast tumor model, that predicted the clinical situation, showing that local tumor size changes rhythmically during each estrous cycle and that the cycling speed modulates average tumor growth rate. Furthermore, we demonstrate that this rhythmic tumor biology is not limited to breast cancer and occurs in another mouse strain with chemically induced transplantable sarcoma.

MATERIAL AND METHODS

Animals and Tumors. The fertility cycle dependent growth characteristics of two different tumors in young cycling female mice were studied in five studies; three studies in an estrone binding, primary transplantable MTP mammary cancer in C_3HeB/FeJ female mice (n= 40, 120, 100 mice/study), [10] and two studies in a primary transplantable methylcholantherene-induced (meth A) sarcoma (E. Caswell, NY) in CD_2F_1 mice (n=16, 86 mice/study). Mice were maintained on a lighting schedule with 12 hours light alternating with 12 hours of dark. Time of day (circadian time) is referenced to hours after light onset (HALO) with lights on at 0 HALO and light off at 12 HALO. Tumors cells were inoculated subcutaneously into the right flank and three dimensional tumor size (TS = length x width x height) was measured by calipers from the time of tumor appearance until sacrifice. Vaginal smears were obtained from mice at the time of tumor inoculation and at each tumor evaluation by gently flushing the vaginal os with saline and then fixing and staining the resultant cells with hematoxylin/thiazine (Diff Quick). Tumor measurements and estrous smears were obtained every 24 hours during the early activity phase (14 HALO) in three studies and every 12 hours during early sleep phase (2 HALO) and again in the early activity (14 HALO) in two studies. In two of the C3H breast tumor studies, tumor-bearing mice were sacrificed at the time of final tumor measurement and the uteri were procured, trimmed of fat and wet weights determined. Tumors from these mice were assessed for wet-to-dry ratios as a function of estrous stage at the time of sacrifice by weighing tumors before and after dissecation of tissue in an 80 degree centigrade drying oven.

Fertitlity Cycle Determintations. Sequential estrous smears were evaluated for each mouse and classified, based upon cellular ratios, abundance of cornified epithelial cells, polymorphonuclear cells and non-cornified epithelial and the findings on the preceding and subsequent smears, into 1 of 4 stages (P, proestrus; E, estrus; M, metestrus; or D, diestrus) by standard criteria confirmed by previous correlations between vaginal cytology and uterine weight wet and a uterine profileration marker.[11] Mice continue to cycle regularly in the presence of these tumors.[19,20] The ovarian cycle in the mouse (~4-5 days) and the woman (28±7 days) are not strictly comparable throughout all stages. However in both, ultimate follicular maturation ends with mature follicular rupture and ovulation in response to FSH and then LH surges. In murine species during proestrus the LH/FSH surge is accompanied by a surge in progesterone (on top of rising estrogen) and these hormonal events are identifiable by vaginal cytology which demonstrates the proestrus to estrus phase transition at which time ovulation usually occurs.
Not all mice cycle at the same rate (variable cycle lengths) and groups of mice are not synchronized in the appearance of estrous cycle stages. Therefore to compare endpoints in mice at different estrous cycle stages, successive cycle numbers (cycle number 1, 2, 3, etc) and estrous stages within each of these cycles (P1, E1, M1, D1; P2, E2, M2, D2; etc) were assigned starting from the time of tumor inoculation until the last measurement. From these assignments, the total number of estrous cycles completed in a fixed time interval between the time of tumor inoculation and the last day of measurement (e.g cycling frequency), was calculated for each mouse by counting the successive appearances or transitions through the proestrous stage.

Protein Immunohistochemistry: Tumors were fixed in 10% buffered formalin and paraffin embedded. The tissue sections, after deparaffinization and hydration, were (digested using proteinase K (20 ug/ml in PBS) for 20 minutes and washed in PBS twice (pH 7.2) for 5 minutes). Endogenous peroxidase activity was blocked by 3% H_2O_2 in PBS for 15 minutes. Slides were incubated in normal goat serum for 2 hours at room temperature. The primary rabbit polyclonal antibody against estrogen receptor (ER □, 1:400, ER □, 1:200) or progesterone receptor (PR, reactive with both A&B subtypes, 1:400) was applied to sections and incubated overnight at 4^0C. The secondary antibody (goat anti-rabbit IgG) and AB complex (Vectastain ABC kit, Vector Laboratory Inc., Burlingame, CA) were applied for 30 minutes at room temperature, respectively. Between incubations, slides were washed three times (5 min/each) in

PBS. The color was developed by 3, 3'-diaminobenzidine tetrahydrochloride (Peroxidase substrate kit DAB, Vector Laboratory Inc., Burlingame, CA). The sections were finally counterstained with Harris' hematoxylin (Sigma, St. Louis, MO). The same slides were stained without primary antibody as negative controls.

Statistical Analysis. Variance among mean values, across more than two groups (e.g. 4 estrous cycle stages) were contrasted using one way analysis of variance (ANOVA) for repeated measures using the SPSS program. Tumor values are expressed as raw tumor volumes at each successive estrous stage and cycle number and as a percent of the mean of all tumor sizes for each fertility cycle (e.g. %mean tumor volume = TS from a mouse in P1 divided by mean all TS in cycle 1 x 100). Uterine weights are expressed as absolute wet weights at each fertility cycle stage and as the percent of the mean value across all stages. Analysis of tumor volume data against number of estrous cycles completed was performed using a repeated measures growth model with Proc Mixed (SAS version 8.02), where restricted maximum likelihood estimation procedure is used and that it considers the number of cycle group as a fixed effect. The unstructured covariance matrix was used. The effects of number of cycles completed, day, and the interaction of number of cycles and day were evaluated by *F* tests. Depicted values are the mean ± standard error for grouped data from individual mice.

RESULTS

Not Unlike the Uterus, Tumor Size Waxes and Wanes Throughout the Fertility Cycle

The fertility cycle stage of tumor inoculation did not affect the time to tumor appearance (palpable tumor) or the subsequent rate of tumor growth over time in the C3H breast tumor or meth A sarcoma (data not shown). Daily tumor size in both models increases in a typical sigmoid dependent pattern when fertility cycle stage is ignored. However, when C3H breast tumor size is serially assessed as a function of biologic time (estrous cycle stage and cycle number) of measurement, the influence of fertility cycle stage upon tumor growth is apparent by visual inspection of average tumor sizes (Figure 1A, Table 1). By grouping animals according to each serial stage of each serially completed estrous cycle regrouped, and examining average tumor sizes as a function of cycle number and stage, we find that tumor size waxes in metestrus and diestrus and wanes during proestrus and estrus. This effect is

consistent across three separate studies of the C3H breast tumor. Virtually identical results are seen in two studies with transplantable methylcholanthrene A induced sarcoma (meth A sarcoma) in CD_2F_1 mice (Figure 1B, Table 1). These changes in tumor size with fertility cycle stage in each tumor type were seen when tumor measurements, along with vaginal smears, were monitored either during the early sleep phase (2 HALO) or during the early activity phase (14 HALO) of the 24 hour circadian cycle of the mice (data not shown). Therefore this estrous biology is present both in the activity and sleep phases of the daily cycle.

Analysis of raw tumor size by both cycle number (e.g. first, second, third, fourth, fifth) and estrous cycle stage within each cycle (P1, E1, M1, D1; P2, E2 etc.) by two way analysis of variance confirms the significance of this phase locked tumor growth in the C3H breast tumor and in the CD_2F_1 meth A sarcoma tumor models. Tumor sizes during each fertility cycle can also be expressed as percentage of the mean tumor size for that cycle in each of the studies, and then analyzed by one way ANOVA for the overall effect of estrous cycle stage (Table 1). In the C3H breast tumors, tumor sizes are 23-47% of cycle mean size during proestrous, increase gradually throughout both estrous and metestrous stages to a peak of 207-283% of the mean in diestrus, varying on average some 6.4 to 8.9 fold throughout the fertility cycle ($p<0.001$). In the meth A sarcoma, tumor sizes are 50-59% of mean cycle size during proestrus, increase gradually throughout both estrus and metestrus stages to a peak of 149-185% of mean cycle size in diestrus, varying on average some 2.5 to 3.7 fold throughout the fertility cycle ($p<0.001$). This rhythmic variation in tumor size follows the identical pattern in both tumors, with highest values in diestrus and lowest values in proestrus or estrus, although the magnitude of this cyclic effect is about twice as great in the mammary tumor. This tumor behavior is not unlike the classically described waxing and waning of uterine size or wet weight that occurs throughout each fertility cycle, secondary to the well described rhythmic sex hormone changes in cellular proliferation and blood content. In these C3H tumor-bearing mice, wet uterine weights in two studies, expressed as percent of mean cycle weight, vary 1.5 to 2.0 fold throughout the fertility cycle with highest values, as expected, in proestrus and estrus, and lower values in metestrus and diestrus (Table 1, $p < 0.01$). However, the pattern of change in tumor size within the fertility cycle is opposite to the

pattern of the observed fertility cycle dependent change in wet uterine weights in these tumor-bearing mice.

Analysis of wet-to-dry ratios as a function of estrous cycle stage at sacrifice (study 2 C3H breast tumor) failed to show significant difference ascribable to water content (proestrus 6.4±0.3 estrus 6.7±0.3)metestrous (6.6±0.2)diestrus (6.5±0.1)($p=0.73$). These data indicate that large fluid shifts are not soley responsible for these tumor size differences.

Both the MTP mammary tumors and the methA sarcoma tumors stain positively for estrogen receptor alpha, negative with estrogen receptor beta and positive for the progesterone receptor (data not shown) by standard immunohistocehmical analysis.

Cycling Frequency of the Host Modulates Overall Tumor Growth Rate

The normal menstrual cycle duration varies among women from 21 to 36 days.[3] Some mice also cycle faster than others with a range of 3 to 7 days.[3] We determined the effect of cycle length upon tumor growth. The faster the mouse cycles, the slower the tumor growth, and vice versa (Figure 2A and 2B). Average tumor growth is reproducibly slower in mice completing a greater number of cycles in a fixed span (e.g. 4 to 7 cycles in 12 to 14 days) while tumor growth is faster, nearly double that rate, in mice completing fewer cycles (e.g. 3 or fewer cycles) in the very same span. These tumor growth rate differences are significant in both strains (C3H $F=5.3$, $p<0.001$; CD_2F_1 $F=4.9$, $p=0.001$).

In study two, we determined whether the effect of cycle stage on tumor growth was present among both slow and fast cyclers. Table 2 demonstrates that the effect of cycle stage on tumor size persists regardless of cycling speed.

DISCUSSION

We have shown that the growth of two transplanted subcutaneous tumors, a spontaneously arising, sex hormone receptor competent, potentially metastatic breast tumor, and a chemically-induced locally aggressive sarcoma, grown in two distinct mouse strains, is virtually identically coordinated by the fertility cycle. These data indicate that the fertility cycle influence over tumor biology and the host-cancer balance is not limited to tumors of endocrine tissue origin and is thereby a phenomenon of more general significance. Whether this behavior exists in ER negative and/or PR negative tumors remains to be determined. The fertility cycle stage

dependent change in tumor size is analogous to the cycle dependent change in uterine size, but has a tissue specific exact opposite pattern in these same mice. The speed of the estrous cycling also affects average tumor growth rate. Faster cyclers demonstrate twofold slower tumor growth than slower cyclers. These data are consistent with epidemiologic findings relating menstrual cycle length and breast cancer risk. Faster cycling is associated with the lower subsequent breast cancer risk.[4,5]

Others have observed similar biology of human breast cancer. One hundred sixty-eight years ago, A.P. Cooper, who defined Cooper's ligaments of the breast, observed that breast cancer growth waxes and wanes regularly within the young women's menstrual cycle.[21] More than a century ago, G.T Beatson connected breast size and milk production to the ewe's 28 day fertility cycle.[22] When Beatson was made professor of surgery as Glasgow, he acted upon his observations of the connection between ovary and breast, by performing oophorectomy upon young women with lethal metastatic breast cancer. His reports were the first of many in the last century to document the fact that breast cancer can be controlled and even caused to remit entirely, following castration.[23] In 1959 through the 1980's, Fisher and Fisher defined the biology of tumor dormancy and demonstrated how the resection of the primary tumor affects the biology of metastatic breast cancer spread.[10,24,25] A decade and a half ago, we demonstrated, in cycling mice and women, that whether breast cancer spreads/recurs after resection depends upon when in the estrous or menstrual cycle the resection is done. Aggregate clinical data indicate that optimal resection timing, mid cycle and during the early luteal phase, gives a young woman as much as a 25% better chance for ten year disease free survival.[15,26] This waxing and waning of tumor size and growth rate within the fertility cycle in mouse breast cancer, and a chemically-induced mouse sarcoma, is entirely consistent with what Cooper reported in the breast tumors of young women. This biology reflects the essentially intermittent or saltatory nature of growth, a cyclical rather than linear or continuous process. This biologic growth pattern is not unique nor unprecedented. Growth studies in children using serial height determinations also provide support for periods of growth interspersed with periods without significant changes in height [27]. Further, in normal reproductive tissues (e.g. breast, uterus), rhythmic periodic changes of cell proliferation and apoptosis are classic findings during each fertility cycle. There is evidence that cellular proliferation in benign human neoplasms also change within the menstrual cycle [28]

Prominent daily rhythms in cellular proliferation have been well documented in murine and human cancer.[29-31]

In summary, both fertility cycle stage and cycling frequency affect the growth of two different experimental cancers across two unrelated mouse strains. If these findings, which are consistent with early clinical observation, remain clinically relevant, then, the effect of the menstrual cycle on cancer growth and spread, may be a general one, not limited to breast cancer. Finally, the timing of cytotoxic hormonal and molecular anti-cancer therapies targeting cellular proliferation within the fertility cycle is likely to affect their efficacy.

REFERENCES

1. Adami H, Sparen P, Bergstrom R, Holmberg L, Krusemo U, Ponten J. Increasing survival trend after cancer diagnosis in Sweden 1960-1984. *J Natl Cancer Inst* 1989;**81:**1640-1647.
2. Adami H, Bergstrom R, Holmberg L, Klareskog L, Persson I, Ponten J. The effect of female sex hormones on cancer survival; a register-based study in patients younger than 20 years at diagnosis. *JAMA* 1990;**263:**2189-2193.
3. Knobil E, Neill J, eds. The Physiology of Reproduction. New York: Raven Press, 1994.
4. Whelan EA, Sandler DP, Root JL, Smith KR, Weinberg CR. Menstrual cycle patterns and risk of breast cancer. *Am J Epidemiol* 1994;**140**(12)**:**1081-90.
5. Magnusson C, Persson I, Baron J, Ekbom A, Bergstrom R, Adami H. The role of reproductive factors and use of oral contraceptives in the aetiology of breast cacner in women aged 50 to 74 years. *Int J Cancer* 1999;**80:**231-236.
6. Lindsey W, Gupta T, Beattie C. Influence of the estrous cycle during carcinogen exposure on nitrosomethylurea-induced rat mammary carcinoma. *Cancer Res* 1981;**41:**3857-3862.
7. Ratko T, Beattie C. Estrous cycle modification of rat mammary tumor induction by a single dose of N-methyl-N-nitrosourea. *Cancer Res* 1995;**45:**3042-3047.
8. Nagasawa H, Yanai R, Taniguchi H. Importance of mammary gland DNA synthesis on carcinogen-induced mammary tumorigenesis. *Cancer Res* 1976;**36:**2223-2226.
9. Pascual R, Hwang S, Swanson S, Bauzon M, Guzman R, Nandi S. c-Has-ras activation in MNU induced rat mammary cancers is regulated by ovarian hormones. *Proc Amer Assoc Cancer Res* 1994;**35:**262.
10. Fisher B, Fisher ER. Experimental evidence in support of the dormant tumor cell. *Science* 1959;**130:**918-919.
11. Bove K, Lincoln DW, Wood PA, Hrushesky WJ. Fertility cycle influence on surgical breast cancer cure. *Breast Cancer Res Treatment* 2002;**75**(1)**:**65-72.
12. You S, Li W, Kobayashi M, Xiong Y, Hrushesky WJ, Wood PA. Creation of a stable mammary tumor cell line that maintains fertility cycle tumor biology of the parent tumor. *In Vitro Cell Dev Biol Anim* 2004;**40**(3).
13. Hrushesky WJM, Gruber SA, Sothern RB, et al. Natural killer cell activity: Age, estrous- and circadian-stage dependence and inverse correlation with metastatic potential. *J Nat Cancer Inst* 1988;**80:**1232-1237.
14. Hrushesky WJM, Bluming AZ, Gruber SA, Sothern RB. Menstrual influence on surgical cure of breast cancer. *Lancet* 1989;**ii:**949-952.
15. Hrushesky W. Breast cancer, timing of surgery, and the menstrual cycle: call for prospective trial. *J Women's Health* 1996;**5**(6)**:**555-565.
16. Hagen A, Hrushesky W. Menstrual timing of breast cancer surgery. *Am J Surg* 1998;**104:**245-261.
17. Love RR DN, Dinh NV, Shen T, Havighurst TZ, Allred DC, et al. Mastectomy and oophorectomy by menstrual cycle phase in women with operable breast cancer. *Journal of the National Cancer Institute* 2002;**94:**662-669.
18. Hrushesky W. Letter to the Editor RE: Mastectomy and Oophorectomy by Menstrual Cycle Phase in Women with Operable Breast Cancer (Love, et al). *Journal of the National Cancer Institute* 2002;**94**(22).

19. Ratajczak HV, Sothern R, Hrushesky WJM. Single cosinor analysis of vaginal smear cell types quantifies mouse estrous cycle and its alteration by mammalian adenocarcinoma. In: Reinberg A, Smolensky M, Labrecque G, eds. Ann. Rev. Chronopharm. New York: Pergam Press, 1986: 223-226.
20. Wood P, Waldo S, Hrushesky W. Lack of major effect of tumor growth and fluoropyrimidine treatment upon maintenance of fertility cycling. In: Touito Y, ed. Biological Clocks: Mechanisms and Applications. Amsterdam: Elsevier, 1998: 507-510.
21. Cooper A. Practice and Principles of Surgery. London: E. Cox, St. Thomas's St., Southwark, 1836.
22. Beatson G. PhD Dissertation, Beatson Cancer Institute. *Beatson Library, Glassow, Scotland.*
23. Beatson G. On the treatment of inoperable cases of carcinoma of the mamma: Suggestions for a new method of treatment with illustrative cases. *Lancet* 1896;**ii:**104-107.
24. Fisher B, Gunduz N, Saffer EA. Influence of the interval between primary tumor removal and chemotherapy on kinetics and growth metastases. *Cancer Res* 1983;**43:**1488-1492.
25. Fisher B, Gunduz N, Coyle J, Rudock C, Saffer E. Presence of a growth-stimulating factor in serum following primary tumor removal in mice. *Cancer Res* 1989;**49:**1996-2001.
26. Fentiman I, Gregory W, Richards M. Effects of menstrual phase on surgical treatment of breast cancer. *Lancet* 1994;**344:**402.
27. Lampl M VJ, Johnson ML. Saltation and Stasis: A Model of Human Growth. *Science* 1992;**258:**801-803.
28. Kawaguchi D, Fujii S, Konishi I, Nanbu Y, Nonagaki H, Mori T. Mitotic activity in uterine leiomyomas during the menstrual cycle. *Am J Obstet Gynecol* 1989;**160:**637-641.
29. You S, XiongY, Kobayashi M, Wood P, Bickley S, Simu M, Quiton J, Hrushesky WJ. Tumor cell circadian clock genes are rhythmically expressed in coordination with rhythmic circadian growth and, thereby, may represent new therapeutic targets. *Clin. Cancer Res.* 2003;**9**(16)**:**6126s.
30. Hori K, Zhang Q-H, Li H-C, Saito S. Variation of growth rate of a rat tumour during a light-dark cycle: correlation with circadian fluctuations in tumour blood flow. *Br J of Cancer* 1995;**71:**1163-1168.
31. Hrushesky W, Lannin D, Haus E. Evidence for an ontogenetic basis for circadian coordination of cancer cell proliferation. *J Nat Cancer Inst* 1998;**90**(19)**:**1480-1484.

Figure 1A

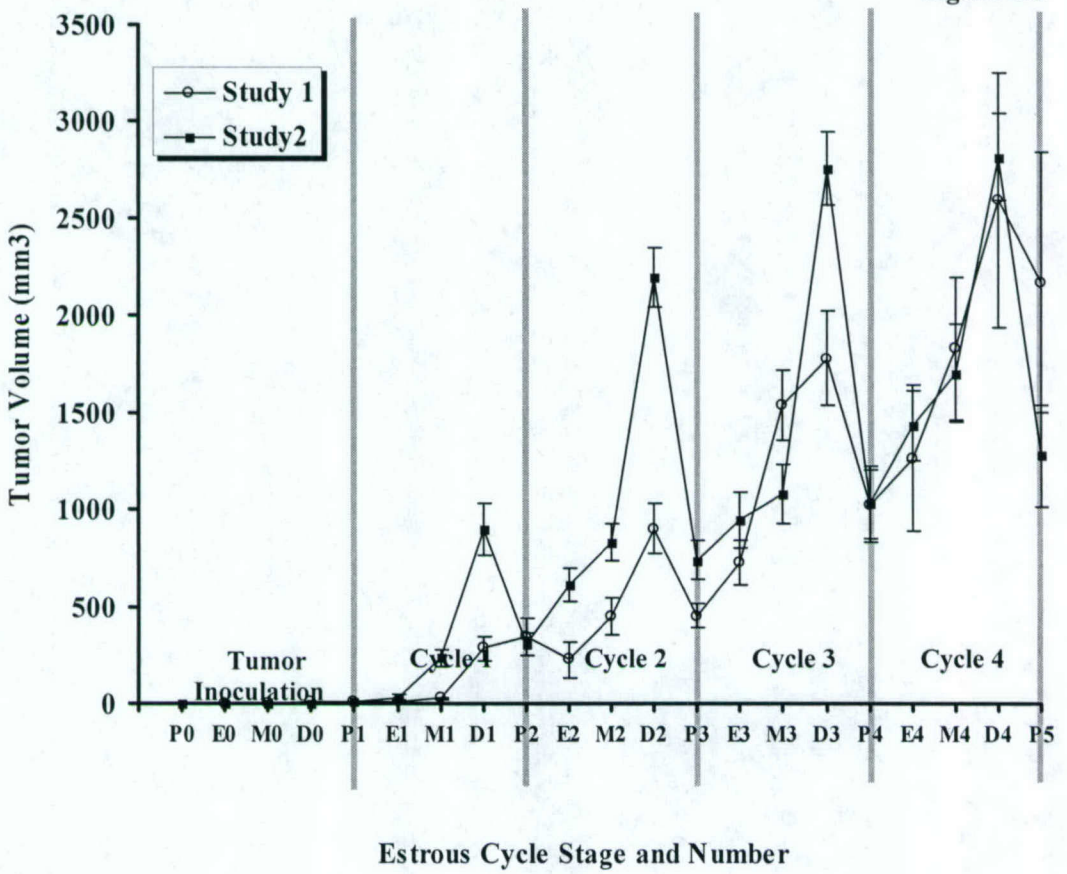
Study 1
Study2
Tumor Volume (mm3)
3500
3000
2500
2000
1500
1000
500
0
Tumor Inoculation
Cycle 1
Cycle 2
Cycle 3
Cycle 4
P0 E0 M0 D0 P1 E1 M1 D1 P2 E2 M2 D2 P3 E3 M3 D3 P4 E4 M4 D4 P5
Estrous Cycle Stage and Number

Figure 1B

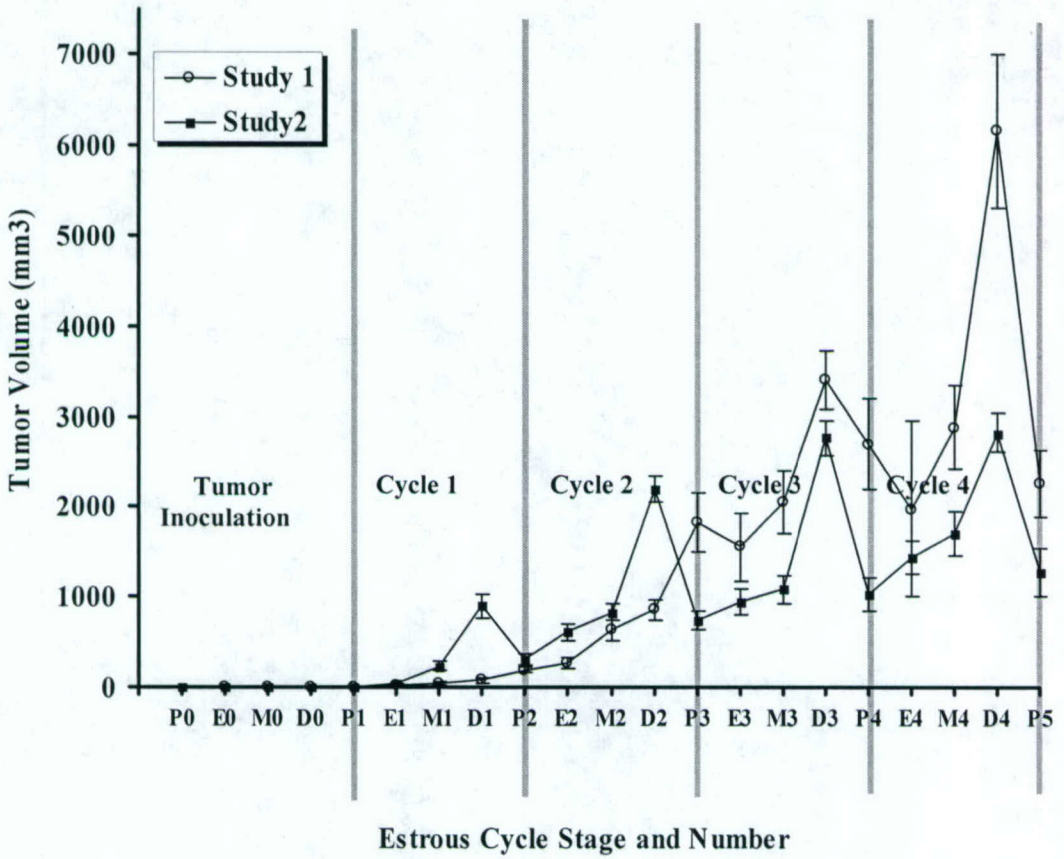
Study 1
Study2
Tumor Volume (mm3)
7000
6000
5000
4000
3000
2000
1000
0
Tumor Inoculation
Cycle 1
Cycle 2
Cycle 3
Cycle 4
P0 E0 M0 D0 P1 E1 M1 D1 P2 E2 M2 D2 P3 E3 M3 D3 P4 E4 M4 D4 P5
Estrous Cycle Stage and Number

Figure 2A

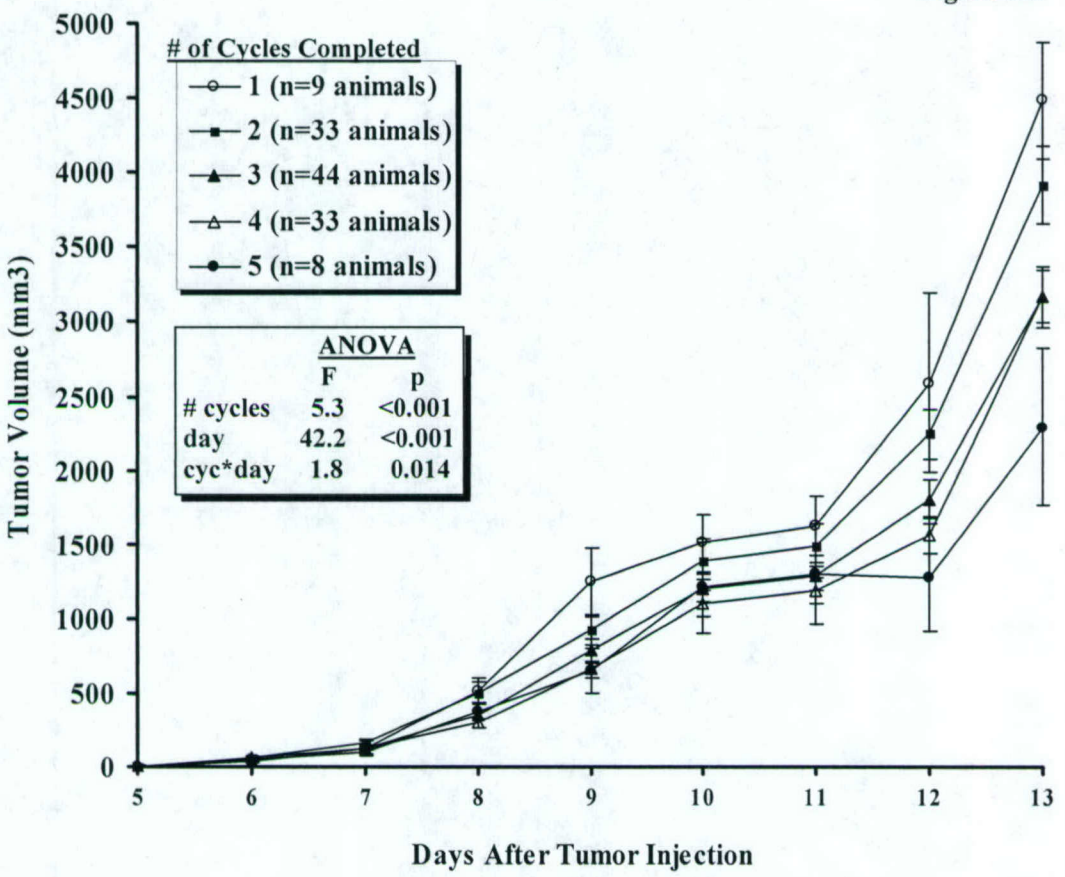
# of Cycles Completed
1 (n=9 animals)
2 (n=33 animals)
3 (n=44 animals)
4 (n=33 animals)
5 (n=8 animals)
ANOVA
F p
cycles 5.3 <0.001
day 42.2 <0.001
cyc*day 1.8 0.014
Tumor Volume (mm3)
5000
4500
4000
3500
3000
2500
2000
1500
1000
500
0
5
6
7
8
9
10
11
12
13
Days After Tumor Injection

Figure 2B

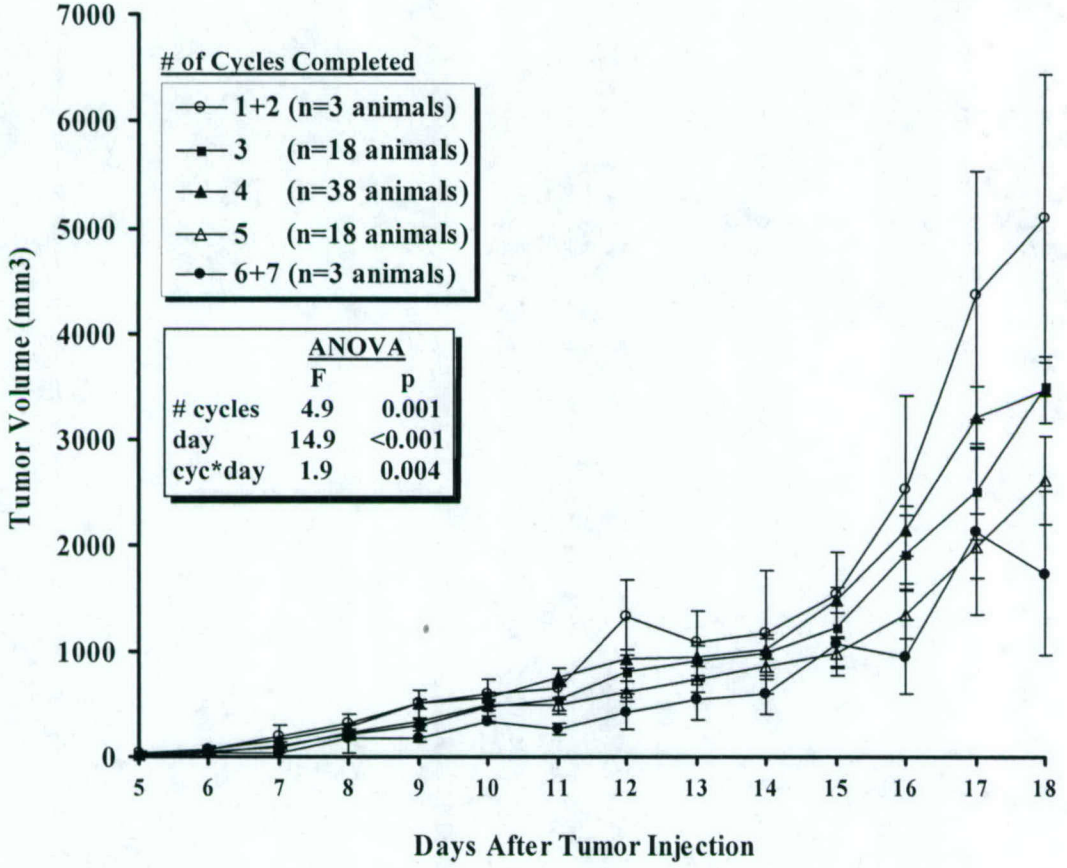
# of Cycles Completed
1+2 (n=3 animals)
3 (n=18 animals)
4 (n=38 animals)
5 (n=18 animals)
6+7 (n=3 animals)
ANOVA
F p
cycles 4.9 0.001
day 14.9 <0.001
cyc*day 1.9 0.004
Tumor Volume (mm3)
7000
6000
5000
4000
3000
2000
1000
0
5 6 7 8 9 10 11 12 13 14 15 16 17 18
Days After Tumor Injection

FIGURE LEGENDS

Figure 1. The effect of estrous cycle stage upon tumor size. Subcutaneous mammary tumor volumes in C_3HeB/FeJ female mice (**A**) and meth A sarcoma tumor volumes in CD_2F_1 female mice (**B**) vary as a function of fertility cycle stage (P, proestrus, E, estrous, M, metestrsous, D, diestrous) during each successive fertility cycle (cycle 0 or tumor inoculation to cycle 4) in two studies. Tumor sizes change rhythmically with fertility cycle stage in both tumor models with very little increase in tumor sizes during proestrus and estrus stages and large increases during metestrus and diestrus stages.

Figure 2. The effect of host cycling frequency upon tumor growth rates. Individual mice were classified by number of completed fertility cycles (1-7 cycles) in the same time interval and tumor growth rates are compared in each model of mammary tumors in C_3HeB/FeJ female mice (**A**) and meth A sarcoma tumors in CD_2F_1 female mice (**B**). The number of fertility cycles traversed significantly affects tumor growth rates in both tumor models.

Table 1. Effect of Fertility Cycle Stage and Cycling Frequency upon Tumor Size and Growth Rate

	Fertility Cycle Stage						Cycling Frequency
	Tumor Size (% Mean of Each Cycle)						*Daily Tumor Growth Rate*
TUMOR MODEL	**Proestrus**	**Estrus**	**Metestrus**	**Diestrus**	**Ratio of Change**	***F, p***	***F, p***
C3H BREAST TUMOR							
Study 1	46.9±7.5	37.8±7.1	73.2±7.9	**219.5±29.7**	5.8	24.2, <0.001	5.4, 0.001
Study 2	23.4±2.4	38.2±3.6	72.8±6.3	**207.1±13.6**	8.9	86.3, <0.001	5.3, < 0.001
5 cycles (n=8)	88.85±25.1	79.6±31.0	99.6±47.3	**137.1±30.5**	0.0	NS	
4 cycles (n=33)	69.3±15.0	73.0±14.3	71.0±13.8	**167.8±21.2**	2.4	8.8, <0.001	
3 cycles (n=44)	56.1±9.2	73.3±11.6	69.5±9.8	**170.5±15.7**	3.0	18.8, <0.001	
2 cycles (n=33)	43.5±9.7	50.1±9.8	70.8±10.2	**193.0±18.8**	4.4	27.3, <0.001	
1 cycle (n=9)	4.4±3.4	16.3±6.7	71.5±17.3	**219.4±32.6**	50.0	18.3, <0.001	
Study 3	44.3±6.5	50.4±7.6	82.6±9.8	**282.7±69.5**	6.4	15.1, <0.001	4.9, 0.001
CD2F1 METH A SARCOMA							
Study 1	50.22±7.1	61.4±14.9	105.2±15.4	**184.6±33.6**	3.7	9.4, <0.001	3.2, 0.043
Study 2	58.6±4.2	76.1±6.4	121.4±17.1	**149.1±26.2**	2.5	6.9, p<0.001	4.9, 0.001
UTERUS	*Uterine Wet Weight (% Mean of Cycle)*						
C3H Tumor Bearing Mice							
Study 2	150.1±21.5	**168.4±5.7**	118.6±5.7	88.0±2.4	1.9	41.6, <0.001	
Study 3	**125.3±11.0**	107.0±4.9	88.1±4.6	104.1±7.2	1.4	4.4, 0.006	

For each succesive fertility cycle (cycle 1, 2, 3, etc), tumor volume at each stage within a given cycle (e.g. P1, E1, M1, D1, etc) is expressed as percentage of the mean tumor volume for all stages within that one cycle. Uterine wet weights at each ferti